

FILE COPY
NO. 2

N 62 57654

★ NACA TM 65

120113

TECHNICAL MEMORANDUMS

NATIONAL ADVISORY COMMITTEE FOR AERONAUTICS

[REDACTED]

[REDACTED]

STRESSES PRODUCED IN AIRPLANE WINGS BY GUSTS

By Hans Georg Küssner

Zeitschrift für Flugtechnik und Motorluftschiffahrt
Vol. 22, Nos. 19 and 20, Oct. 14 and 28, 1931
Verlag von R. Oldenbourg, München und Berlin

Reproduced by
NATIONAL TECHNICAL
INFORMATION SERVICE
US Department of Commerce
Springfield, VA. 22151

[REDACTED]

[REDACTED]

Washington
ary, 1932

PRICES SUBJECT TO CHANGE

NATIONAL ADVISORY COMMITTEE FOR AERONAUTICS

TECHNICAL MEMORANDUM NO. 654

STRESSES PRODUCED IN AIRPLANE WINGS BY GUSTS*

By Hans Georg Küssner

Whereas, in calm air, the stresses in an airplane wing depend on the airplane characteristics and on the pilot, the latter has little or no influence on the magnitude of such stresses in gusty weather from the point of view of maintaining flight schedule and cruising speed. Consequently, this airplane must be able to withstand such stresses in any case.

The first information on stresses in gusts was collected by W. Hoff in 1914.** At that time there was no need to attach any special significance to such stresses, because the speed range of the airplane, i.e., the ratio of maximum speed in uniform level flight to stalling speed was, in most cases, essentially lower than 2, and flying was, in the main, confined to fair weather. But since that time the airplane has undergone enormous changes and improvements until to-day air transportation has developed until it is practically imperative to fly under bad as well as good weather conditions.)

In order to gain a comprehensive conception of the flow phenomena in the open air, let us first glance over some meteorological reports:

1. Official entry of telephone conversation with weather forecasting station, Tempelhof, Oct. 10, 1929:

"At this station the following vertical velocity components of gusts have been recorded:

Normal (on cumulus clouds),	2 to 4 m/s	656/10-10-12
Very frequently in bad weather zones,	6 to 8 m/s	1968/10-26-24
Rare maxima,	12 " 13 m/s	3936/10-24-64

(Signed) Thalau."

*"Beanspruchung von Flugzeugflügeln durch Böen." Zeitschrift für Flugtechnik und Motorluftschiffahrt, Oct. 14, 1931, pp. 579-586; and Oct. 28, 1931, pp. 605-615.

**Technische Berichte der Flugzeugmeisterei, Vol. I, 1917, p. 61.

2. Letter from German Naval Observatory, Meteorological Research Institute, to the D.V.L., October 25, 1929:

"In answer to your request, we submit the latest reports of our forecasting station:

No exact measurements on the vertical velocity in gusts are available at this post. We can only give approximate values based upon our experiences in numerous flights in clouds and gusts.

The most violent bumps are always encountered at the front of an advancing gust roller, while at its upper border and above it the intensity is much abated. In this respect only gust fronts with cold air inflow areas are being considered. The order of magnitude of the vertical up and downward velocity components varies between 5 and 20 m/s.

Sidling into or flying through a cumulus, the strongest gusts are encountered directly at the border of the cumulus; 5 to 10 m/s may be considered as normal for the vertical component of the velocity. Below the Cu. an up current of from 2 to 5 m/s prevails.

In bad-weather zones 5 to 10 m/s velocities have been noted quite frequently. Bad-weather zones accompanied by gusts are most generally bound up with areas of inflow of cold air and with the passing of a convergence.*

15 to 20 m/s are considered rare maximum in gusts. However, it may be assumed that the maximum values of the horizontal components in bad weather may also be those for vertical gusts, so that an extreme of 30 m/s is still within the ambit of possibility.

*See F. Exner, *Dynamische Meteorologie*, Leipzig, 1917, p. 239.

W. Schmidt, *Wiener Sitzungs Bericht*, Vol. 119, 1910, p. 1101.



This information is deduced from airplane meteorograph records. The above experiences are confirmed by aerological data from pilot balloon ascensions. The figures cited are valid for dynamic pressures within the first few kilometers above the ground.

(Signed) Unterschrift."

3. A. Lohr, Cloud Flying:*

"The view of a convection cumulus field is much more imposing. The Cu. formations of the convection space evince a much mightier form of towering head than the Cu. of the friction space; they rise lofty into the sky and conjure, through their sharp contrast in light and shadow effect, miraculous, magnificent pictures. Towering from their midst are lofty thunderheads, reaching upward as high as 6000 meters. The pronounced bumpiness at the border of such towering heads is, of course, well known. But the warning against attempts to fly through them cannot be emphasized enough. They are invested by vertical gusts of from 10 to 15 m/s velocity, whereas beneath an ordinary Cu. formation the uprush of the air is not expected to be more than 2 to 4 m/s and which, of late, is so successfully utilized in sailing flight. Closely related to the vertical current with up-welling Cu. heads are the caps over the Cu., which to a large extent are ice formations and risen stratus layers penetrated by the towering head. The latter spread out and often rise along the flanks of the tower. From time to time veil-like stratus clouds are pushed up by the turbulent layer beneath, making one feel as though being above a smooth stratus layer in which the cumulus fields with soft fountain forms are imbedded."

"Another important object in cloud flying is the observation of the restlessness of the air within and in the neighborhood of clouds. One case in point is the restlessness of the air in the van of a gust. Obviously, flight within or below it is avoided. But frequently we started ahead of the oncoming roller. It was found that in a spread of from 3 to 5 km in the van of the gust some very pronounced vertical

*Meteorologische Zeitschrift, 1930, September issue.

gusts do exist which, however, vanish immediately after one passes directly above the gust roller, where the space directly behind the gust head, in particular, is very calm."

O. Lange, The Aerological Conditions in Cumulus Clouds:*

"Although the entire descent was made with idling engine, the instruments recorded practically the same altitude for 20 seconds at 3000 meters, and a gain of over 100 meters in 40 seconds at 2500 meters, which can only be explained as being due to vertical movements in the air. The sinking velocity of the airplane from 4800 to 3000 meters is 540 meters per minute, and from 2600 to 1200 meters, it is 530 meters per minute, or approximately 9 m/s. According to this, the upwind at 3000 meters is about 8 m/s, and 12 m/s at 2500 meters. In between, the vertical velocity is from 2 to 3 m/s.

Recapitulation: The records reveal that the air bodies of cumulus clouds by "following weather" are colder than the surrounding air. Within the cloud, a fairly humid adiabatic gradient holds sway, the inversions and isotherms of the vicinity are destroyed by the turbulence, but a stronger inversion at greater heights acts as barrier layer. The vertical motion does not extend uniformly over the whole cloud but fluctuates horizontally; the maximum recorded upwind velocity is 12 m/s. Around zero temperature considerable ice formed on the airplane; below zero we encountered hail. Aside from pressure spots on the propeller the airplane, being all-metal, showed no visible damage. But the whole flight demonstrated that it cannot be emphasized enough not to fly through thunder clouds." (Compare the altitude time curve No. 4.)

*Beiträge zur Physik der freien Atmosphäre, 1930, No. 2.

5. Georgii, The Airplane as Medium for Aerological Research:*

"The weather conditions of the flights on July 30, 1929, are characterized by the occlusion of a "low," shifting during the night of the 29th from the coast of the North Sea toward the Pomeranian coast. The flights were made in the very unstable cold air bodies behind the front. The instability of the atmosphere was manifested by pronounced cumulus clouds (8/10 cu.) throughout the whole day which, without connection to distinct fronts was indubitably due to the strong turbulence of the brisk west wind. The upwind flights this day are typical of the existing vertical motions in such cumuli. We have the records from three sailplanes: the "Luftikus," pilot Bedau, at 12.11 p.m., the "Wien," pilot Kronfeld, at 3.30 p.m., and the "Rhoadler," pilot Groenhoff, at 5.25 p.m. which, in spite of the difference in the hours, show many common symbols of the vertical motion. The "Wien" shows an almost uninterrupted climb from take-off at 950 m up to 3000 m, first in the dynamic upcurrent of the Wasserkuppe, then from 1500 m on in the uprush of a cumulus entered after leaving the mountain slope. The cumulus was traversed from base to top, so the vertical velocities at 1600 to 3000 m height correspond to the rising air current in the cumulus. The maximum (5 m/s), was reached between 2200 and 2700 m. One surprising feature of the three flights is a distinct abatement in the ascending air current at around 1400 m altitude. The record of the "Wien" showed only a short bend in the altitude-time curve, whereas in the "Luftikus" it manifested at this height longer variations in up- and-down wind, very similar to those in the "Rhoadler," but of course, of decidedly shorter period within the same level. The very violent vertical gusts encountered at 1800 m, according to Groenhoff's record, are particularly illuminating.

Between the 51st and 53d minute of flight the airplane was pushed down 140 m in a few seconds and pulled up again 170 m in the next. Two other similar but less violent bumps followed immediately.

*Beitrage zur Physik der freien Atmosphere, 1930, No. 3.

The shock and the torsion were so severe that it tore the plywood covering over the fitting of the wing to the fuselage. The evaluation of the gusts reveals a descending air current of 9 m/s, and an ascending current of 10 m/s where, of course, it should be borne in mind that these velocities still represent averages, even if only for a period of from 10 to 20 seconds. The altitude-time curve of the "Luftikus" also discloses marked fluctuations in vertical current for this day. The upwind velocity jumps at between 1200 and 1500 m altitude also within a very few seconds, from +4.1 to +0.8, then to +4.7, and again to +1.2 m/s. This is suggestive of the existence of very material vertical currents in cumulus clouds, even if they do not develop into cumulus nimbus, and their importance in aviation is far from secondary because airplanes and chiefly airships are subject to enormous stresses in such short-period vertical gusts.* (Compare altitude-time curves Nos. 5 and 13.)

6. Georgii, Report on 11th Rhön Glider Meet:*

"Bedau first sailed in the upwind of the Wasserkuppe; in the 214th minute of his flight he connected with the upcurrent of a cloud which carried him at moderate rate of climb to 1600 meters absolute altitude. After the first rise the upcurrent in the cloud abated, then suddenly in the 226th minute an abnormally powerful and wholly unexpected current clutched the airplane and lifted it over 900 meters within 3 minutes. The sudden rise was followed by a drop in which the rate of descent increased to approximately 25 m/s, which later changed into spiral flight, in which Bedau then emerged from the cloud. On the basis of 0.7 m/s sinking velocity for the "Luftikus," the vertical velocity in the cloud ranged between 6 and 7 m/s. This rising air current in an ordinary cumulus of around 1200 m ambit is very great. It exceeds the previously measured vertical velocities considerably and demonstrates more clearly the existence of vertical movements in ostensibly harmless appearing clouds which, ordinarily, are not suspected outside of storm

*Zeitschrift für Flugtechnik und Motorluftschiffahrt, Vol. 22, No. 5, 1931, p. 131.

clouds. The unexpected station shift from very low vertical motion to great ascending velocities, as evidenced by Bedau's barogram in the 226th minute, leads us to surmise that the upwind in the cumulus is caused by an eddy with horizontal or even vertical axis, and the air currents on a mountain slope offer many possibilities to generate such eddies." (Compare altitude-time curve No. 1.)

7. Moltchanoff, Structure of Squalls in the Open Atmosphere* (Measurements on Horizontal Gusts; the Structure of Vertical Gusts is Fundamentally Similar):

"The records from kites indicate the general duration of each gust at from 0.2 to 0.3 second, although in isolated cases, gusts up to 12 seconds have been recorded. Figure 1 shows one of such kite records. The gust lasted about 4 seconds. At present we are making contemporary studies of gusts at different heights." (See fig. 1.)

8. W. Schmidt, The Structure of the Wind:*

"In the summer of 1928 we were able to explore a field of about 10 X 10 m in 25 different test stations on the Aspern airport in Vienna. The test spacing (2 m), of course, was so wide that the smallest interferences escaped, but it brought out the major changes only more clearly. The place was favorable; we exercised great care in having the wind pass over the field to the observer's post which was placed far enough away from all buildings so as to give the wind a clean sweep (surrounding is farmland). The best of the 17 series, on July 24, 12.14 p.m., sunny, very hot (over 30°C), wind N.W., comprises 300 records, represented in exactly the same manner as Podersdorf's series (real instantaneous isotachs).

Because of the limited space, we reproduce only sections of it. The individual pictures are 1/7 s. apart; they are given in groups of three at intervals of approximately 1 second in Figure 3.

*Beiträge zur Physik der freien Atmosphäre; 1930, No. 3.
 **Wiener Sitz.-Ber., Vol. 138, 1929, p. 100; Deutsche Forschung, 1930, No. 14, p. 58.

This large cross section substantiated the deductions drawn previously: marked variation in flow velocity vertically and horizontally, frequently faster moving layers beneath slower ones, practically no sign of a real eddy (at least, not of the order of magnitude of several meters), entry of rapidly moving masses. New information was gained with respect to the transformation of such masses, which in this case arrive usually in a more horizontal direction, but subsequently appear to straighten up. The surprising feature is that the strongest contrasts of the velocity in such bumps follow so closely along one another; two meters farther the velocities may be as smooth as 1:4 without producing a proper equalization."

9. K. Wegener, Application of Flight Weather Observations:*

"The gustiness reported by an airplane may be the result of three different causes. Two air strata stably superposed but moving in different directions evince billows along their boundaries like those generally seen where water and air meet. These aerial billows have just as little regularity as the sea billows and are felt in the airplane as violent bumps - bumpiness. They are readily recognized as such because they occur only in a comparatively thin layer which rarely exceeds 100 to 300 meters thickness.**

A second form of bumpiness is that encountered when the air is turbulent; it is similar to the irregular, eddying motion of a river. This motion is recognized in the airplane by its rapid changes but not such pronounced bumps.

The third form of bump is caused by the vertical exchange of air. Cold air flowing over comparatively warm ground becomes heated, rises, and cold air from above takes its place. This exchange is usually strongest by N.W. to N. wind. It may attain ver-

*Der Flugkapitän, 1930, No. 11.

**F. M. Exner, Dynamische Meteorologie, Leipzig, 1917, p. 278, where he cites a wave length of 441 m for a 5 m/s difference in velocity and 10°C difference in temperature. Handbuch d. Techn. Mechanik, Vol. VI, Berlin, 1928, p. 240.

tical velocities up to 15 m/s, although it makes flying almost impossible even at from 5 to 10 m/s, with the sluggish and inherently stable airplanes of today, because of the tiring effect on the pilot. The prevalence of this kind of bumpiness is contingent upon the temperature gradient being greater than $0.01^{\circ}\text{C}/\text{m}$ by dry air, so that the air is in "stable" equilibrium. The first two kinds of bumps present no real danger to flying unless the airplane has about reached its ceiling, that is, has no surplus power left."

WING STRESSES IN GUSTS

The author and his collaborator Kaspereit have made a series of optigraph measurements of such stresses with the Junkers G 24, F 13, and the Messerschmitt M 24 in 25 flying hours. The method has already been described elsewhere.* The installation into the fuselage and below the center section of the wing can be seen in Figures 13 and 23, while Figures 14-16, 24, and 25 show some sections of the records. Figures 3, 17, 19, 26 represent merely some of the most typical cases.

In the Messerschmitt M 24 we used two optigraphs for recording the deflection of the wing over the whole span. In this manner errors induced by shifting of the instrument are more easily eliminated. The maximum static deflection of the wing tips in flight with full gross weight amounts to about 95 mm as compared to the normal position of the wing on the stand. The maximum dynamic deflection of the wing in sun gusts during a five-hour flight from Berlin to Friedrichshafen amounted to within ± 35 mm. (See fig. 3.)

In the Junkers F 13 the static deflection in flight, 8.85 m from the center of the fuselage with full gross weight, amounted to 75 mm as compared with the normal position on the stand. The maximum dynamic deflection for a flight over the Marker Sea in bright sunlight was 52 mm at 300 m altitude. (See figs. 17, 19, 25.) To compute the load factors the static deflection of the wing for its own weight would have to be determined and subtracted from the total deflection. This could be accomplished by

*Küssner, Zeitschrift für Flugtechnik und Motorluftschifffahrt, 1930, Vol. 21, p. 433.

disposing the whole airplane on an incline, an investigation which is to be made later.

The low stresses in distinctly stormy weather are surprising.

After several such measurements have been obtained, particularly of bad weather flights, the ratio: dynamic deflection to flight speed is plotted against the logarithm of the frequency and gives, by extrapolating according to Gauss' law of distribution, a criterion for the requisite strength of the wing.

We also examined the fine structure of several optograms recorded in the M 24, the F 13, and the G 24. We measured the variation of the deflection of the extreme station on the wing with respect to the time. (See figs. 6 to 12, 18, 20, and 27.) From the interval of the rise of the deflection to maximum, and the shape of the lines of rise, we can draw conclusions about the structures of gusts. (Compare section on Unsteady Wing Lift, page 14.)

NOTATION

a_0 to a_4	coefficients of the differential equation (23).
A_1 A_2 A_3	integration constants (equation 25).
α	angle of attack.
α_0	angle of attack for maximum lift coefficient (equation 7a).
b	m semispan.
C	1. integration constant, 2. coefficient of gust stress, C_1 minimum value for strength calculation (equation 26).
$c_a' = \frac{dc_a}{d\alpha}$	variation in lift coefficient with angle of attack.
c_1	circulation factor (equation 5).

$\gamma = \frac{1}{w_0} \frac{\partial w}{\partial s}$	1/m	gradient of gust velocity (equation 15a)
$\eta(s), \eta_0(s)$		coefficients of unsteady lift; η_m , $\eta_{0,m}$ = time rate of averages (equation 11).
e		basis of natural logarithm.
$f(z) = \frac{F(z)}{g}$	s^2	elastic line of deflection by acceleration 1 m/s ² .
F	m ²	wing area.
F(z)	m	true elastic line of deflection.
ϕ		direction of gust with respect to the horizontal (equation 6).
$\Phi(h, s)$		function of starting point distance (equation 1).
g	m/s ²	acceleration of gravity.
G	kg	gross weight of airplane.
h	s ²	1. displacement of zero point (equation 22).
h s	m	2. distance of starting point from the source of motion for computing the circulation (equation 1).
$i = \sqrt{-1}$		fictitious unit.
k	kg s/m ³	factor (equation 20).
K	kg	normal load on the wing (equation 2).
K_0	kg	maximum normal load preceding separation of profile flow (equation 7).
K_0'	kg	maximum normal load at separation of flow (equation 7a).
K_s	kg	normal load in steady level flight (equation 7b).

κ (s)		diminution factor (equation 4).
l	m	wing chord.
λ_1, λ	1/s	roots of the typical equation (24).
m	$\frac{\text{kg s}^2}{\text{m}^2}$	mass/unit of length.
m'	$\frac{\text{kg s}^2}{\text{m}^2}$	vibrating mass (wing mass and co-vibrating air cylinder (equation 20)).
M_D	kg m	turning moment around the forward neutral point (at 1/4 wing chord) (equation 3).
μ		mass ratio (equation 13a).
n		load factors (equation 8).
n_0		load factors for vertical gust.
n_{B_r}		critical load factor.
n_s		(maximum) load factor for pull-up.
v	1/s	basic frequency of wing in flight.
v_0	1/s	basic frequency of wing on stand.
$r = \gamma v$	1/s	exponent of velocity increase of gust.
$r_2 = \frac{F}{4 b^2 \pi}$		coefficient of induced drag (equation 5).
ρ	$\frac{\text{kg s}^2}{\text{m}^4}$	air density.
s, s_1		relative flight path = ratio of flight path to wing chord.
s_0		path on which the velocity of the gust increases linearly from 0 to maximum (equation 15a).
t	s	time.

$U(s) = \frac{\mu \ddot{y}}{v w_0}$	ratio of actual to computed gust stress by assumed steady flow and rectilinear motion (equation 13a).
U_0	maximum for $U(s)$ (equation 7).
v	m/s flying speed.
v_h	m/s maximum horizontal speed.
v_L	m/s stalling speed. (Landing speed) (equation 9)
v_P	m/s velocity of rear neutral point (at 3/4 of wing chord) (equation 1)
\underline{w}	m/s vectorial velocity of gust (equation 6).
w_0	m/s absolute value of gust velocity (equation 6); w_0' in a descending gust (equation 15).
w_i	m/s ideal normal velocity.
w_m	m/s mean horizontal wind velocity (equation 6).
$w(s)$	m/s 1. velocity component perpendicular to plate surface. m/s 2. vertical velocity of the air (gust) with respect to flight path.
ω	1/s angular velocity.
ω_i	1/s ideal angular velocity.
$\xi = w_0/v$	velocity ratio (equation 8a).
y	m displacement of one wing element perpendicular to direction of flight.
$\ddot{y}_0 f(z)$	m deflection of elastic wing.
$\psi(s) = \frac{w_i}{w_0}$	(equation 11)

z m coordinate in direction of wing span.

$\zeta = \frac{\ddot{y}_0^{\text{elastic}}}{\ddot{y}_0^{\text{rigid}}}$ elastic overstress = ratio of maximum dynamic stress in an elastic wing to that in a rigid wing.

UNSTEADY WING LIFT *Wagner*

H. Wagner,* in his dissertation, gave a general analysis of the dynamic lift of airplane wings in unsteady motion.

Assume a flat plate of chord l and span ∞ moves at velocity v_p , varying periodically in time and direction, through the fluid, and simultaneously rotates at periodically changing angular velocity ω . Further, let v_p represent the velocity of the rear neutral point P (in $3/4$ wing chord), α the angle of attack between the direction of v_p and that of the plate; the fluid in ∞ is assumedly at rest, all angular changes are small and point O is the source or starting point of the unsteady motion. (See fig. 28.)

Then let**

$$w(s) = v_p \sin \alpha = \frac{1}{\pi} \int_0^1 \Phi(h s) \sqrt{1 + s - h s} \frac{d h}{\sqrt{h - h^2}} \quad (1)$$

be the component of the velocity perpendicular to the plate surface.

Now the normal load acting on the plate is

$$K = \pi \rho v_p w - \frac{\rho v_p}{2} \int_0^1 \frac{\Phi(h s)}{\sqrt{1 + s - h s}} \frac{d h}{\sqrt{h - h^2}} + \frac{\pi \rho}{4} \frac{d w}{d t} - \frac{\pi \rho}{16} \frac{d \omega}{d t} \quad (2)$$

*H. Wagner, Zeitschrift für angewandte Mathematik und Mechanik, 1925, pp. 17-35.

**Insert in the formulas of the thesis: $\alpha = h \cdot s$ and $u(\alpha) \sqrt{\alpha} = \phi(h \cdot s)$.

The moment about the forward neutral point D (at 3/4 wing chord), counted tail heavy when positive, moreover, is

$$M_D = - \frac{\pi \rho}{16} v_p \omega - \frac{\pi \rho}{16} \frac{d\omega}{dt} + \frac{\pi \rho}{128} \frac{d\omega}{dt} \quad (3)$$

Now in order to define the function $\phi(hs)$ express the distance of starting point A from the motion source

$$hs \leq 1 \text{ by the function } \phi(hs) = \sum a_m (hs)^m$$

$$hs \geq 1 \text{ " " " } \phi(hs) = \sum a_m (hs)^{-m}$$

and bring both sides of equation (1) into approximate agreement.

An approximate solution for normal velocity $w(s) =$ constant, that is, a sudden inferior change in α , has been given by H. Wagner.* In this case the integral of equation (2) is

$$\Delta K = \rho v_p w \kappa(s),$$

wherein the diminution factor

$$\kappa(s) \sim \text{arc cot } \frac{s}{2}$$

is to within 6.6 per cent correct. The exact figures are appended in Table I.

Table I. Unsteady Lift

s	0	0.25	0.5	1	2	5	10	∞
$1 - 1/\pi \text{ arc cot } s/2$.5	.5396	.5780	.6476	.7500	.8788	.9371	1
$\eta = 1 - 1/\pi \kappa(s)$.5	.5557	.6006	.6693	.7582	.8745	.9321	1
$\eta_0(s)**$	0	(.450)	.572	.652	.749	.871	.931	1

* Zeitschrift für angewandte Mathematik und Mechanik, 1925, p. 31.

** See equation (11), p. 21.

In the general case of arbitrary velocity change, which may be visualized as consisting of a multitude of small abrupt changes, the normal load then is

$$K(s_1) = \pi \rho v_p w(s) - \rho v_p \int_0^{s_1} \kappa (s_1 - s) \frac{dw}{ds} ds + \frac{\pi \rho}{4} \frac{dw}{dt} - \frac{\pi \rho}{16} \frac{d\omega}{dt} \quad (4)$$

The first term represents the steady lift in undisturbed flow which, in airplane wings, is lowered by the effect of the finite span and the skin friction. So instead of factor π we write the lift coefficient* as

$$\frac{c_a'}{2} \sim \frac{c_1}{1 + 2 r_2 c_1} \sim 2.3 \quad (5)$$

It is to be assumed that the skin friction effect is still further reduced by the other unsteady terms of equation (4), in so far as the motion has its inception at $\alpha = 0$. But, since this condition is not complied with in most cases, that is, vortex trains already exist, the value given in (5) is introduced in all terms. An experimental check of the validity of these assumptions, although very much to be desired, is difficult to carry through. However, in no case is it permissible to express coefficient c_a' as the lift change of the whole airplane or as a value in the neighborhood of the separation of flow, but always by a mean value for the airplane wing.

STRESSES IN AIRPLANE WINGS BY GUSTS

FROM ARBITRARY DIRECTIONS

The movements of the air masses quite frequently extend unsymmetrically from the ground to several thousand meters, as the weather reports, cited at the beginning of this report, clearly indicate. The mean horizontal wind velocity w_m is topped by a gust vector

$$\underline{w} = w_0 e^{i\varphi} \quad (6)$$

*See Zeitschrift für Flugtechnik und Motorluftschiffahrt, 1928, p. 516, for comparison. For conventional wing sections $c_1 \sim 2.5$ to 2.9 . Factor $r_2 = F/4\pi b^2$ corresponds to the aspect ratio of the wing.

with a possible amplitude of from $w_0 \sim 0.5$ to $1.0 w_m$. At the customary flying height - 1000 to 2000 meters - all angles ϕ of the gust direction with the horizontal are probable; the disturbances in the uniform air motion in this case may be construed as turbulent rollers. The air loads on an airplane wing flying into a gust are about the same as those caused by sudden changes in angle of attack and air speed in calm air. In spite of the fact that the above stated postulate of the fluid at rest at infinity no longer holds for this problem of the flow, appreciable discrepancies with respect to the above problem are only to be expected during the time of entry of the wing into the turbulent ball bounded by an area of discontinuity.

In view of the scarcity of information on atmospheric air movements and of the mathematical difficulties, an approximate application of the previously achieved results to the wing in agitated fluid should be of interest.

To get some conception of the effect which direction ϕ of the gust vector exerts on the stress in an airplane wing, it suffices to make a rough calculation of the maximum normal load for the time after the entry of the wing (relative flight path $s > 1$). The velocity w within the gust is assumedly invariable while passing from 2 to 5 wing chords where the maximum stress usually occurs. It is also presumed that the longitudinal inclination of the airplane with respect to the horizontal does not change. Consequently, the normal load must be computed from the first two terms of equation (4). According to the assumption (6) regarding the gust vector, the effective horizontal velocity is $v_p = v + w_0 \cos \phi$, and the normal velocity is $w = v \sin \alpha + w_0 \sin (\alpha + \phi)$. (See fig. 28.) Thus the maximum normal load on the wing is

$$K_0 \sim \pi \rho v_p w - \pi \rho v_p (1 - U_0) \int_0^s \frac{dw}{ds} ds$$

$$\sim \pi \rho (v + w_0 \cos \phi) (v \sin \alpha + U_0 w_0 \sin (\alpha + \phi)) \quad (7)$$

The factor U_0 is exactly computed elsewhere. Its numerical value is 0.6 to 0.7; Table II was compiled with mean value $U_0 \sim 2/3$.

Now let $\sin \alpha_0 \sim 0.3$ represent the angle of attack at which the steady flow separates. Stipulating that the

separation also occurs for unsteady flow at the same angle α , the normal load, on the other hand, cannot grow beyond

$$K_0' \leq \pi \rho v^2 (1 - U_0) \sin \alpha + \pi \rho v_p^2 U_0 \sin \alpha_0 \quad (7a)$$

The maximum acceleration of the airplane in multiples of acceleration of gravity, called load factor, now is obtained by dividing (7) and (7a) by the steady lift

$$K_s = \pi \rho v^2 \sin \alpha, \quad (7b)$$

which equals the individual weight of the airplane. Expressing the ratio of the velocities by $\frac{w_0}{v} = \xi$ and $\sin \alpha \sim \tan \alpha$, since it is always a matter of small α , the load factor according to (7) and (7a) now becomes:

$$n \leq (1 + \xi \cos \varphi) \left(1 + \xi U_0 \cos \varphi + \xi U_0 \frac{\sin \varphi}{\sin \alpha} \right) \quad (8a)$$

$$n \leq 1 - U_0 + U_0 \frac{\sin \alpha_0}{\sin \alpha} (1 + \xi \cos \varphi)^2 \quad (8b)$$

Table II contains several illustrative examples of load factors computed in this manner.

Table II. Load Factor of Gust Stress
with Respect to Angle of Gust

ξ	$\sin \alpha$	$\varphi=0$	10°	20°	30°	40°	50°	60°	70°	80°	90°
0.2	0.133	1.36	1.56	1.74	1.90	2.01	2.09	2.13	2.12	2.08	2.00
		-	-	-	-	2.32	2.24	2.15	2.04	1.94	1.83
"	0.100	1.36	1.63	1.88	2.09	2.26	2.38	2.45	2.46	2.41	2.33
"	0.067	1.36	1.77	2.15	2.48	2.76	2.96	3.08	3.13	3.09	3.00
"	0.050	1.36	1.91	2.42	2.87	3.25	3.54	3.72	3.80	3.77	3.67
0.3	0.100	1.56	2.00	2.40	2.74	2.99	3.17	3.25	3.24	3.15	2.99
		-	-	-	3.51	3.36	3.18	2.98	2.76	2.55	2.33
0.4	0.100	1.78	2.40	2.97	3.45	3.81	4.04	4.11	4.08	3.92	3.66
		-	-	-	3.97	3.76	3.50	3.21	2.93	2.62	2.33

The lower figures of the series indicated by } are occasionally valid and have been plotted against angle of gust φ in Figures 29 and 30. The maximum load factor is reached at $\varphi \sim 65$ to 70° , although it differs but little (not over 10 per cent) from that at $\varphi = 90^\circ$, that is, load factor n_0 produced by a vertical gust. Moreover, the numerical value of n_0 can be used for estimating the maximum stress even if the corresponding flow attitude is no longer realized as a result of separation, because the intersection of the two curves (8a) and (8b) yields a value which differs but little from the load factor n_0 , although for smaller φ .

By given flying speed, that is, prescribed steady angle of attack $\sin \alpha$, control maneuvers without speed increase, that is, pull-up from horizontal flight, do not produce a load factor higher than

$$n_s = \frac{\sin \alpha_0}{\sin \alpha} = \frac{v^2}{v_L^2} \quad (9)$$

wherein v_L is the minimum sustaining speed in unstalled flight (landing speed).

It is worth mentioning that according to recent flight tests by the D.V.L.* the angle α_0 of the separation of flow in flight can be essentially higher than for model tests in the tunnel.

The speed of present-day airplanes is, with few exceptions, at least $v = 40$ m/s or more. On the other hand, it can be assumed that a gust velocity of more than $w_0 = 15$ m/s is seldom exceeded, so that the velocity relation

$$\xi = \frac{w_0}{v} \leq 0.4 \quad (9a)$$

may be assumed. According to Figure 30 the load factor given by (9) for $\xi = 0.4$ in oblique gusts cannot be exceeded by more than 25 per cent. This figure is practi-

*F. Seewald, Zeitschrift für Flugtechnik und Motorluftschiffahrt, Vol. 22, No. 13, 1931, pp. 405-410. According to recent wind-tunnel tests of Mr. Kramer at the Aachen Institute, the angle stalling by unsteady flow increases by $\Delta \alpha_0 \sim \frac{5l}{v} \frac{dw}{dt}$.

cally unaffected by the size of load factor n_g . Then if we estimate the overstress of the wing (calculated further on) by the loading impact (swinging beyond the equilibrium position) at approximately 20 per cent, we obtain a rough upper limiting value for the possible load factor in gusts:

$$n \leq 1 + 1.2 \left(1.25 \frac{v^2}{v_L^2} - 1 \right) \sim 1.5 \frac{v^2}{v_L^2} \quad (9b)$$

The question of requisite strength and safety factor is purposely left open. For high-speed airplanes the assumption (9a) is too unfavorable, so that condition (9b) is likewise not always fulfilled. (See fig. 46.)

This type of airplane must be studied more in particular for gusts of limited amplitude, say, $w_0 = 10$ to 15 m/s. In view of the other sources of error of the calculation it amply suffices to compute these airplanes for a vertical gust, since no materially higher stresses are possible in other directions of gusts. But in a calculation of this kind the separation of the flow must not be taken into account.

EQUATIONS OF MOTION AND STRESS ON AIRPLANES IN VERTICAL GUSTS, PLANE PROBLEM

To begin with, picture an airplane as rigid wing with ∞ span and mass m per unit length uniformly distributed over the span. The previously cited omission of changes in inclination of the longitudinal axis of the airplane against the horizon is permissible because the wing is raised only a few centimeters with respect to the tail surfaces, at the beginning of entry into the gusts. As soon as the tail surfaces have penetrated, they are raised much quicker by the gust than the wing because of their much more reduced mass, so that the initially slight rise in angle α is already on the decline at the time of the maximum stress. The introduction of the longitudinal inclination in the subsequent formulas, however, entails no fundamental difficulties.

With the above assumptions it is now possible to simulate the effect of the vertical gust on the wing by attributing to it an ideal angle of attack change. Suppose the wing flies at constant speed v and $\alpha = 0$ from calm

air vertically into an area of discontinuity, behind which the air has the constant vertical velocity w_0 . Considered physically, a steady increase in normal load and moment is anticipated. This, evidently, is the case when conformably to (3) and (4)*

$$M_D = \frac{\pi \rho}{16} \left[-v \dot{w}_i - \dot{w}_i + \frac{\dot{\omega}_i}{8} \right] = 0 \quad (10)$$

$$\Delta K = \frac{\pi \rho}{4} \left[\dot{w}_i - \frac{\dot{\omega}_i}{4} \right] = 0$$

Taking into account that the relative flight path is $s = vt/l$, equation (10) reveals the ideal angle of attack change the wing would have to make by steady shift into the gust. The corresponding ideal normal velocity is

$$\dot{w}_i = \frac{\dot{\omega}_i}{4} = C e^{-ss}$$

$$w_i = w_0 (1 - e^{-ss}) = w_0 \psi(s).$$

According to (4) the normal load becomes:

$$\begin{aligned} K &= \pi \rho v w_0 (1 - e^{-ss_1}) - \rho v w_0 \int_0^{s_1} \kappa (s_1 - s) \frac{d\psi(s)}{ds} ds = \\ &= \pi \rho v w_0 \eta_0(s_1). \end{aligned} \quad (11)$$

The new factor $\eta_0(s)$ is given in Table I. Now the normal load on the wing by arbitrary change of the vertical air velocity $w(s)$ is readily computed from (11) because

$$K = \pi \rho v \int_0^{s_1} \eta_0 (s_1 - s) \frac{dw}{ds} ds \quad (12)$$

is analogous to (4) and (11).

The third and fourth terms in (5) disappear conformably to (10) as long as the wing moves along a straight line without turning. But as soon as the wing makes an accelerated movement through the unsteady aerodynamic

*Abbreviation: $\dot{x} = \frac{dx}{dt}$; $\dot{\omega} = \frac{d\omega}{dt}$; $\ddot{y} = \frac{d^2y}{dt^2}$.

loads acting upon it, the additive air load must be computed according to (4).

So, when disregarding the rotation, and denoting the wing mass by m and the vertical component of the wing motion by y , the integral equation of the flight path for an airplane of chord l passing from calm air into a vertical gust is

$$\begin{aligned} \left(m + \frac{\rho c_a'}{8}\right) \ddot{y} + \frac{\rho v c_a'}{2} \int_0^{t_1} \eta(s_1 - s) \ddot{y} dt &= \\ &= \frac{\rho v c_a'}{2} \int_0^{t_1} \eta_0(s_1 - s) \dot{w} dt \end{aligned} \quad (13)$$

With the abbreviation:

$$v t = s; \quad \frac{2m}{\rho c_a'} + \frac{l}{4} = \mu; \quad \frac{\mu \ddot{y}}{v w_0} = U(s) \quad (13a)$$

Equation (13) then becomes:

$$U(s_1) + \frac{1}{\mu} \int_0^{s_1} \eta(s_1 - s) U(s) ds = \frac{1}{w_0} \int_0^{s_1} \eta_0(s_1 - s) \frac{dw(s)}{ds} ds \quad (14)$$

The new variable $U(s)$ gives the ratio of the true to the calculated stress by assumed steady flow and linear motion. This presumption is approximately correct for a wing having ∞ mass after a certain entering distance necessary to set up the steady circulation. Consequently, $U(s)$ likewise expresses the ratio of the true stress of an airplane with finite mass to that of an airplane of ∞ mass.

The total load normally acting on the wing inclusive of static lift is according to (7):

$$K = \frac{\rho v^2 c_a'}{2} \sin \alpha + \frac{\rho v w_0 c_a'}{2} U(s) \cos \alpha \quad (14a)$$

The desired maximum of $U(s)$, that is, the maximum wing stress in the gust, can be graphically determined by iteration from the integral equation (14), after making the necessary assumptions regarding the local distribution of the gust intensity $w(s)$.

Judging from the reports of Moltchanoff and W. Schmidt, the gradient of the velocity can assume values of the order of

$$\gamma = \frac{1}{w_0} \frac{\partial w}{\partial s} = 0 \text{ to } 1.5 \text{ [1/m]},$$

or, in other words, the violence of the gust can rise from 0 to maximum even within a flight distance of $1/\gamma \sim 0.7$ m. This is less than one wing chord and already approaches a sudden change in gust intensity as previously assumed for the calculation of factor η_0 , despite the fact that only steady transitions in the atmosphere and finite values of gradient γ are physically feasible. The most elementary case, which occurs rather frequently, is the linear rise in vertical velocity from 0 to a constant maximum w_0 . (Compare fig. 1.)

Assume for the flight path

$$\left. \begin{aligned} s = 0 \text{ to } s_0: \quad w = \frac{w_0}{s_0} s; \quad \frac{dw}{ds} = \frac{w_0}{s_0} \\ s = s_0 \text{ to } s_1: \quad w = w_0; \quad \frac{dw}{ds} = 0 \end{aligned} \right\} \quad (15)$$

wherein the path along which the velocity increases is:

$$s_0 = \frac{1}{\gamma} \quad (15a)$$

The integrals in (14) really contain, so to speak, the entire antecedents of the wing motion as well as the after effect of previously traversed gusts. For instance, the wing may have attained a downward velocity w_0' through a descending gust. In this case, according to (15), we have

$$\begin{aligned} s = 0 \text{ to } s_0 \left(1 + \frac{w_0'}{w_0}\right): \quad w = \frac{w_0}{s_0} s; \quad \frac{dw}{ds} = \frac{w_0}{s_0} \\ s = s_0 \left(1 + \frac{w_0'}{w_0}\right) \text{ to } s_1: \quad w = w_0 + w_0'; \quad \frac{dw}{ds} = 0, \end{aligned}$$

and now we must insert the inferior limit,

$$s_1 - s_0 \left(1 + \frac{w_0'}{w_0}\right)$$

in the integral on the right side of the subsequent equation (15b) so as to include the approximate previous effect of the descending gust. An exact integration of (14) for a longer flight distance would consume too much time and be abortive at that, because of our lack of information on the structure of gusts.

Now (14) becomes through (15)

$$U(s_1) + \frac{1}{\mu} \int_0^{s_1} \eta(s_1 - s) U(s) ds = \frac{1}{s_0} \int_{s_1 - s_0}^{s_1} \eta_0(s) ds \quad (15b)$$

which yields the maximum U_0 given in Figure 32 as functions of the path $s_0 = 1/\gamma l$ and of the mass ratio μ .

The values of $U_0 \leq 0.8$ occur within the technical range.

$$\text{The formula: } w = w_0 (1 - e^{-s/s_0}) \quad (16)$$

embraces very rapid as well as very slow increases in gust velocity from 0 to w_0 in a function which for $s = 0$ and ∞ subtends the curves of formula (15). (See fig. 31.) Writing (16) into (14), we obtain:

$$U(s_1) + \frac{1}{\mu} \int_0^{s_1} \eta(s_1 - s) U(s) ds = \frac{1}{s_0} \int_0^{s_1} \eta_0(s_1 - s) e^{-\frac{s}{s_0}} ds \quad (17)$$

This integral equation yields as solution a similar behavior of the maximum U_0 values as with (15) (fig. 33); but they are lower than in the first formula because of the steady decrease of gradient γ for equal values of s_0 (fig. 32).

For very small gradients γ , that is, for very slow rise in gust, the maximum stress is attained only after a flight path $s_1 > 10$. Even then the integrals of (14) can still be divided without appreciable error into

$$U(s_1) + \frac{\eta_m}{\mu} \int_0^{s_1} U(s) ds = \eta_{0m} \frac{w(s)}{w_0} \quad (17a)$$

Setting $U(s) = \lambda e^{\lambda s}$ the left side as linear differential equation, yields the root

$$\lambda = - \frac{\eta_m}{\mu}$$

Figure 34 illustrates the approximate course of the averages η_m and η_{0m} for linear increase in vertical velocity $w(s)$ and for stress $U(s)$. At $s > 10$ both averages are already > 0.8 . Writing these values as well as (16) into (17a) and further considering that $U = 0$ for $s = 0$ also, we find

$$U(s) \sim \eta_{0m} \frac{e^{-\frac{\eta_m}{\mu} s} - e^{-\frac{s}{s_0}}}{1 - \frac{s_0 \eta_m}{\mu}}$$

The maximum stress is reached after covering distance

$$s_1 = s_0 \frac{\ln \frac{\eta_m s_0}{\mu}}{\frac{\eta_m s_0}{\mu} - 1}$$

The result is the figures in Table III, for the maximum stress U_0 , which is materially affected by the gradient γ of the gust velocity or, in other words, by the distance s_0 of the gust increase. Therefore, it is just as important to gain more accurate information on the gust gradient as it is on the gust velocity itself. For the deflection curves recorded during the flight in sun gusts (Berlin to Friedrichshafen) the maximum stress was usually reached only 1-2 seconds after entry; that is, after a distance $s_1 = 15$ to 30 wing chords. (See figs. 6 to 12.) This fact leads us to conclude of very small gradients $\gamma \leq 0.03$ (m^{-1}). Still, the obtained maximum of the vertical velocity can be considerable.

Table III. Effect of Gradient

$\eta_m s_0/\mu$		0.5	1	2	3	5
s_1/s_0 U_0/η_{0m}		1.39	1	0.69	0.55	0.40
		0.501	0.368	0.250	0.193	0.134
$\mu/\eta_m = 10$	s_0	5	10	20	30	50
	s_1	6.9	10	13.9	16.5	20.1
	U_0	0.376	0.294	0.207	0.165	0.119

Consequently, it would be erroneous to conclude on the stress in the wing from the height of the vertical velocity alone. According to (15) airplanes having large wing chord l are subject to higher stresses. The increase in gust intensity is quicker in relation to the chord. On the other hand, it will be remembered that the assumption of plane flow, which forms the basis of this investigation, is more rarely fulfilled in large than in small airplanes, because the gust velocity is likewise variable in direction of the span. (See fig. 2.) It is, indeed, very seldom that all parts of the surface on large wings will be simultaneously subjected to high stresses by gusts. If a gust strikes, say, only one half of the wing, the mass reduced to the center of attack amounts to only about 0.2 of the total mass. (See figs. 32 and 33). But in order to be certain, the most abnormal case, namely, plane flow, must be investigated.

SPATIAL PROBLEM, EFFECT OF ELASTICITY OF WING

Now, we determine the effect of the elasticity of airplane wings on the stress due to gusts. Assumedly, the mass of the airplane is no longer evenly distributed over the span but largely centered in the middle, i.e., in the fuselage. Each wing element is to have plane flow and the lift is to be proportional to the wing chord, a stipulation which corresponds very much to the tapered wings in Figure 35, when overlooking the extreme tips.

The wing is to advance vertically on to a gust stratum, so that both halves of the wings experience the same stresses. Again ignoring changes in inclination of the longitudinal axis of the airplane, we then obtain accord-

ing to (13) the following system of integro-differential equations for the loads and moments impressed on the wing:

$$\int_0^b m' \frac{\partial^2 y}{\partial t^2} dz + k \int_0^b l \int_0^{t_1} \eta (s_1 - s) \frac{\partial^2 y}{\partial t^2} dt dz =$$

$$= k \int_0^b l \int_0^{t_1} \eta_0 (s_1 - s) dw dz \quad (20a)$$

$$\int_0^z m' \frac{\partial^2 y}{\partial t^2} dz^2 + k \int_0^z l \int_0^{t_1} \eta (s_1 - s) \frac{\partial^2 y}{\partial t^2} dt dz^2 =$$

$$= k \int_0^z l \int_0^{t_1} \eta_0 (s_1 - s) dw dz^2 \quad (20b)$$

Herein

$$m' = m + \frac{\rho c_a' l^2}{8}$$

$$k = \frac{\rho c_a' v}{2}$$

For short time intervals (20) can be integrated as linear system, by inserting the mean value

$$\int_0^{\Delta t} \eta (s_1 - s) \frac{\partial^2 y}{\partial t^2} dt = \frac{\partial y}{\partial t} \frac{1}{\Delta t} \int_0^{\Delta t} \eta (s_1 - s) dt = \frac{\partial y}{\partial t} \eta_m(l) \quad (21)$$

The formula

$$y_i = e^{\lambda_i t} (f_i(z) + h_i); \quad f_i(0) = 0$$

yields ∞ fold solutions, of which, however, only three concern us here. The first is an aperiodic motion of the airplane as a whole, where $f_1(z)$ is small with respect to h_1 , and corresponds to the previously described motion of the rigid wing. The second and third solutions yield the fundamental harmonic of the airplane damped by the air loads. The other higher harmonics of the wing are agitated by gusts with only negligibly small amplitude, so that knowledge of them is not essential.

Since this method of solution already involves considerable figuring, it is desirable to arrive at an approximate solution by a short cut, particularly since the

sources of error contained in the above assumptions together with our scant knowledge on gust structure make any great accuracy in calculation appear valueless.

The deflection curves of airplane wings were recorded by optigraph on the following types of airplanes: Do X, G 24, F 13, and the M 24. The form of these curves in one airplane type was almost independent of the absolute size of the deflections in gusts and shows practically no difference from the static deflection curve because fineness in load distribution is blotted out by the fourfold integration which leads to the deflection curve. (See figs. 5 and 22.)

The real static deflection curve $F(z)$ of an airplane can be measured in flight by optigraph, or else satisfactorily reproduced in the hangar by load tests. The fundamental harmonic ν_0 of the wing flutter in flight or static test can be determined in the same way.*

The next thought is to use these two experimental data for computing the gust stress by making the form change of the wing proportional to the static deflection curve and then follow it up by a definition of the total vertical displacement y of one wing element so as to yield the fundamental harmonic of the wing with a frequency ν_0 at $v = 0$.

With $f(z) = \frac{F(z)}{g}$ as the static deflection curve by acceleration 1, this condition is complied with by

$$y = y_0 + \ddot{y}_0 (f(z) + h) \quad (22)$$

when the neutral point displacement is

$$h = \frac{1}{\nu_0^2} + \frac{\int m' f(z) dz}{\int m dz}$$

Thus, the ideal displacement \ddot{y}_0 is the criterion of the dynamic stress in the wing. A static normal load of

$$K = \ddot{y}_0 \int_0^b m dz$$

would be equivalent to it.

*Luftfahrtforschung, Vol. IV, No. 2, and 1929 Yearbook of the D.V.L., p. 513.

If we form (according to (13a)) the ratio $U(s)$ of the actual to the computed stress under assumed steady flow and linear motion, then

$$U(s) = \frac{2 \ddot{y}_0}{\rho v w_0 c_a'} \frac{\int_0^b m dz}{\int_0^b l dz} = \frac{2 \ddot{y}_0 G}{\gamma v w_0 c_a' F}$$

The load factor is

$$n = 1 + \frac{\ddot{y}_0}{g}$$

Combined with formula (22) equation (20a) becomes

$$\begin{aligned} & \left(y + \frac{1}{v_0^2} \ddot{y}_0 \right) \int_0^b m' dz + k \int_0^b l \int_0^{t_1} \eta (s_1 - s) \ddot{y}_0 dt dz + \\ & + k \int_0^b l (f(z) + h) \int_0^{t_1} \eta (s_1 - s) \ddot{y}_0 dt dz = \\ & = k \int_0^b l \int_0^{t_1} \eta_0 (s_1 - s) \dot{w} dt dz \end{aligned} \quad (23)$$

By forming average values conformably to (17a) and (21) for a short time interval, the solution of (23) can be still more simplified. Let

$$\begin{aligned} \eta_m(l) &= \frac{1}{t_1} \int_0^{t_1} \eta \left(\frac{vt_1}{l} - \frac{vt}{l} \right) dt \\ \eta_{0m}(l) &= \frac{1}{t_1} \int_0^{t_1} \eta_0 \left(\frac{vt_1}{l} - \frac{vt}{l} \right) dt \\ a_0 &= k \int_0^b l \eta_{0m}(l) dz \\ a_1 &= k \int_0^b l \eta_m(l) dz \\ a_2 &= \int_0^b \left(m + \frac{\rho c_a' l^2}{8} \right) dz \end{aligned}$$

$$a_3 = k \int_0^b l (f(z) + h) \eta_m(l) dz$$

$$a_4 = \frac{a_2}{v_0^2}$$

Then (23) changes to

$$a_4 \ddot{\ddot{y}}_0 + a_3 \dot{\ddot{y}}_0 + a_2 \ddot{y}_0 + a_1 \dot{y}_0 = a_0 w.$$

The formula $y_0 = e^{\lambda t}$ yields the typical equation

$$a_4 \lambda^4 + a_3 \lambda^3 + a_2 \lambda^2 + a_1 \lambda = 0 \quad (24)$$

with the three roots which are not zero

$$\lambda_1; \lambda_0 + iv; \lambda_0 - iv.$$

For gust increase the formula

$$w = w_0 (1 - e^{-rt}); \quad r = \gamma v$$

is again used, which yields the special solution,

$$\dot{y}_0 = \frac{w_0 a_0}{a_1} + \frac{w_0 a_0 e^{-rt}}{a_4 r^3 - a_3 r^2 + a_2 r - a_1} = \frac{w_0 a_0}{a_1} + \frac{w_0 a_0 e^{-rt}}{N(r)}$$

Now the complete solution of (24) reads as

$$\begin{aligned} \dot{y} &= \frac{A_1}{\lambda_1} e^{\lambda_1 t} + \frac{e^{\lambda_0 t}}{\lambda_0^2 + v^2} [(\lambda_0 A_2 - v A_3) \cos vt + \\ &\quad + (v A_2 + \lambda A_3) \sin vt] + \frac{w_0 a_0}{a_1} + \frac{w_0 a_0}{N(r)} e^{-rt} \\ \ddot{y} &= A_1 e^{\lambda_1 t} + e^{\lambda_0 t} [A_2 \cos vt + A_3 \sin vt] - \frac{w_0 a_0 r}{N(r)} e^{-rt} \\ \ddot{y} &= \lambda_1 A_1 e^{\lambda_1 t} + e^{\lambda_0 t} [(\lambda_0 A_2 + v A_3) \cos vt + \\ &\quad + (\lambda_0 A_3 - v A_2) \sin vt] + \frac{w_0 a_0 r^2}{N(r)} e^{-rt} \end{aligned} \quad (25)$$

In time interval $t = 0$, $y = \dot{y} = 0$, that is, for all z values which, according to (22), is plainly possible only when

$$\dot{y}_0 = \ddot{y}_0 = \dddot{y}_0 = 0.$$

Thus (25) reveals the following determinating equations for the integration constants

$$\frac{A_1}{\lambda_1} + \frac{\lambda_0 A_2}{\lambda_0^2 + v^2} - \frac{v A_3}{\lambda_0^2 + v^2} + \frac{w_0 a_0}{a_1} + \frac{w_0 a_0}{N(r)} = 0$$

$$A_1 + A_2 - \frac{w_0 a_0 r}{N(r)} = 0$$

$$\lambda_1 A_1 + \lambda_0 A_2 + v A_3 + \frac{w_0 a_0 r^2}{N(r)} = 0$$

and therefrom the constants

$$A_1 = - \frac{\lambda_1 w_0 a_0}{N(r)} \frac{N(r) (\lambda_0^2 + v^2) + v^2 + (\lambda_0 + r) a_1}{(\lambda_1 - \lambda_0)^2 + v^2}$$

$$A_2 = - A_1 + \frac{w_0 a_0 r}{N(r)}$$

$$v A_3 = - \lambda_1 A_1 - \lambda_0 A_2 - \frac{w_0 a_0 r^2}{N(r)}$$

In this manner we calculated as examples the types G 24, J 49, F 13, and M 24, and specifically for different gradients γ of gust increase. (See figs. 36-39.) For comparison, we also calculated the accelerations for the same airplanes with assumedly rigid wings ($a_3 = a_4 = 0$). Table IV and Figures 40-43 illustrate the results, which in view of the previously mentioned forming of averages are of comparative value only. Accurate solutions of (20) for different gust forms are reserved for a future report.

Whereas in the rigid wing the effect of the gradient on the stress is no longer great, once it exceeds a certain value ($\gamma l > 0.4$) (compare fig. 33) the elastic wing evinces precisely in the technically important range

of $0.4 > \gamma > 0.1$ (1/m) a marked dependence of the gradient on the stress. Because of the rapidly increasing air loads the wing flies beyond its semistatic equilibrium position and as result thereof increases the total stress considerably. In fact, it can increase to as much as 10 to 70 per cent in the above-mentioned range of γ as compared to the rigid wing. As already pointed out, gust gradients of the order of those in Figures 40-43 are not looked for except in bad weather. Figure 20, for example, shows the damped-out wing flutter of the type calculated. But in the other wings the measured deflection changes occurred so slowly that vibrations were no longer perceptible. (See figs. 6 to 12 and 18.) Therefrom we may conclude of a small gust gradient $\gamma < 0.03$ and an inferior effect of the wing elasticity on the stress.

It is specially unfavorable when the vibration cycle coincides with the time it takes for a rigid wing to attain its maximum stress. In Figure 44 the overstress of the elastic wing with respect to the inelastic wing is plotted against gust gradient γ . Aside from the limiting value $\gamma = \infty$, the overstress ξ of the elastic wing within the practical ambit of γ is so much less as its natural frequency is higher, i.e., the stiffer it is.

In gusts of several seconds' duration the stress in the elastic wing is always higher than in the inelastic wing, even if inferior accelerations are noticeable in the fuselage. According to (22) the acceleration in the fuselage is

$$\ddot{y} = \ddot{y}_0 + h \ddot{y}_0''.$$

Since the ideal acceleration \ddot{y}_0 is the criterion of the stress, this differential equation should first be solved according to \ddot{y}_0 , providing the fuselage acceleration \ddot{y} as time function is known. Inasmuch as this, aside from the uncertainty regarding factor h , would be very tedious, the acceleration measured in the fuselage for computing the wing stress is unsuitable as soon as it becomes a matter of short-time processes.

Physiologically it is explainable that continuous accelerations \ddot{y} in the fuselage are disagreeable to the passengers, a condition which applies more to the cantilever monoplane than to other types. But to conclude herefrom on the magnitude of the actual wing stresses

would be misleading. To illustrate: Although small bumps are even felt in a car well supported by springs, it does not imply that the stress in the springs hereby could not be considerable.

Beyond direct stress measurement on the individual parts, which quite often is difficult on account of thin walls and uncontrollable distribution of stress over the cross section, the most elementary criterion of the actual stress in airplane wings is the deflection curve by optigraph. In view of the perplexing multiplicity of atmospheric flows any precise prediction is fallible, so that for years to come we invariably will have to rely upon the measurement of the stresses in flight and their static interpretation.

Table IV. Approximate Calculation of Gust Stress of Four Airplanes with Respect to Wing Elasticity. Vertical Velocity in $\infty W_0 = 1 \text{ m/s}$

Type	G kg	F m ²	2 b m	v m/s	ρ kg s ² /m ⁴	c_a'	v_0 l/s	v l/s
G 24	6000	89	28.5	56.1	.1075	4.31	16.7	15.9
J 49	4000	91	28.2	44.5	.1053	4.53	18.0	17.7
F 13	1790	43	17.6	35.1	.1150	4.30	27.8	27.7
M 24	2430	43	20.6	37.5	.1150	4.82	37.5	37.2
	a_4	a_3	a_2	a_1	a_0	λ_1	λ_0	$\lambda_1' = -\frac{a_1}{a_2}$
G 24	1.095	3.83	305.8	357.5	357.5	-1.18	-1.16	-1.17
J 49	0.623	3.35	202.0	295.4	295.4	-1.49	-1.94	-1.46
F 13	0.128	0.50	98.8	135.0	127.4	-1.37	-1.28	-1.37
M 24	0.090	0.47	126.0	156.6	149.8	-1.25	-2.02	-1.24
Type	$r=\gamma v$	A_1	A_2	A_3	$a_0 r : N(r)$	A_1'	ζ	
G 24	∞	1.186	-1.186	0.001	0	1.169	1.64	
J 49	∞	1.508	-1.508	-0.038	0	1.462	1.51	
F 13	∞	1.376	-1.376	0.005	0	1.366	1.70	
M 24	∞	1.250	-1.250	-0.026	0	1.243	1.73	
G 24	11.22	1.329	-0.360	-0.612	0.969	1.305	1.68	
J 49	8.90	1.814	-0.244	-0.663	1.570	1.750	1.47	
F 13	7.22	1.602	-0.070	-0.323	1.532	1.590	1.23	
M 24	7.50	1.435	-0.029	-0.237	1.405	1.425	1.16	
G 24	5.61	1.504	-0.102	-0.390	1.402	1.477	1.40	
J 49	4.45	2.268	-0.044	-0.373	2.224	2.178	1.26	
F 13	3.61	2.094	-0.014	-0.168	2.080	2.075	1.14	
M 24	3.75	1.792	-0.003	-0.120	1.789	1.778	1.08	
G 24	2.81	2.046	-0.020	-0.208	2.026	2.002	1.13	
J 49	2.23	4.550	0	-0.190	4.550	4.248	1.10	
F 13	1.80	5.416	0.001	-0.085	5.417	5.307	1.06	
M 24	1.88	3.573	0.002	-0.060	3.575	3.526	1.03	

RECAPITULATION

a) To obtain the maximum stress of an airplane in gusts, it practically suffices to compute its acceleration in vertical gusts. The achieved numerical value then can even be put approximately equivalent to the maximum stress in an oblique gust, when the computed flow attitude in the vertical gust is no longer realized because of "separation."

b) Our knowledge on gust intensity and on gust structure in particular, is sadly lacking, although this phase of research has received considerable attention of late from various sources. Limiting values - about 15 m/s - of gust velocities are sufficiently known, but we lack corresponding information on gust gradients, which is just as important for stress calculations as the gust velocity itself.

c) Accurate prediction of gust stress being out of the question because of the multiplicity of the free air movements, the exploration of gust stress is restricted to static method which must be based upon

1. Stress measurements in free flight;
2. Check of design specifications of approved type airplanes.

With these empirical data the stress must be compared which can be computed for a gust of known intensity and structure. This "maximum gust" then must be so defined as to cover the whole ambit of empiricism and thus serve as prediction for new airplane designs.

d) Taking into account all secondary effects, particularly of gust direction and wing elasticity, the load factor of airplanes in gusts is

$$n = 1 \pm \frac{\rho v_{ca}^2 F}{2G} C \quad (26)$$

The stress coefficient C is a function of the "maximum gust" and of all structural data of the airplane.

The division of C into two factors w and η , of which one is to be solely a function of the free air movement and the other only a function of the structural data

as proposed in the DLA leaflet No. 1, for the D.V.L. specifications is, however, as this consideration shows, no longer feasible.

As long as no mathematical information of the order indicated in section on Equations of Motion and Stress on Airplanes in Vertical Gusts, Plane Problem, was available regarding the dependence of coefficient C on the named variables, only a minimum C_i value could be obtained from the strength of the present airplanes.

According to the hitherto very elementary control of the specifications by stiff load factors, this minimum C_i value together with (26) can be considered a step forward, for at least it gave the correct effect of the flight speed and loading mechanically similar to the load factor.

For that reason the author suggested, anent leaflet No. 1, a proposal to which the safe load factor

$$n = 1 + \frac{1.33 v_h F}{G}$$

corresponded.

Since it may be assumed that the pertinent air density ρ as well as the lift change c_a' is approximately equal for all commercial airplanes, it was accordingly

$$\frac{\rho c_a' C_i}{2} \sim 1.33; \quad C_i \sim 5 \text{ m/s.}$$

The product $0.5 \rho c_a' C$ for a number of approved type German commercial airplanes is given in Figure 45. The factor C_i lies, as seen, on the lower edge of the cluster, therefore is a minimum requirement.

e) Under the presumption that the gust velocity by high gradient never exceeds $w_0 = 15 \text{ m/s} \leq 0.4 v$ in our latitudes; it was possible to indicate - considering wing elasticity and gust direction - an upper limit of the possible load factor

$$n < 1.5 \frac{v^2}{v_L^2} \quad (27)$$

for regular weatherproof airplanes, against whose transgression a definite factor of safety must be provided by special agreement. But instead of the safety factors, considerations on probability of rupture as advanced by Skutsch* could also be used.

It is worthy of note that equation (27) for horizontal maximum speed v_h of all sport, training and acrobatic types of airplanes as well as of 70 per cent of the German commercial types, is complied with, with varying high safety,** and at cruising speed $v_R = 0.85 v_h$, as much as 90 per cent of the commercial types. (See fig. 46.) Possibly the consideration for (27) already gives a competent explanation for the ultimate load factors of airplane wings hitherto arrived at by experience.

At any rate, the maximum stresses in flight, even if occurring rarely, are materially higher than half the ultimate load. The reason these facts do not more often lead to accidents is that "light construction" components, wings also, can, if suitably designed, be loaded several times up to close to their breaking limit, without showing any perceptible damage.***

Very instructive are two failures of the lateral control system which occurred on one and the same airplane type; approved for commercial use for over a year it embodied several aerodynamic improvements over a two-year-old type. The ultimate load of rudder and fin for the new type was about 110 kg/m^2 and about 140 kg/m^2 for the old one. Both accidents were presumably caused by gust impacts of about 13 m/s normal to the control surface. No objections were raised in the old type, although it probably experienced similar stresses in flight.

The flow phenomena in the atmosphere thus prove the deciding factor for the stress in any airplane not de-

*Der Bauingenieur, 1926, p. 915.

**In the range below it three accidents through wing failure occurred within the last year, two on the same type (marked by a cross in Figure 46). Both airplane types represented new constructions of approved older types, greater engine performance, and various aerodynamic improvements, particularly, balanced elevator.

***Development of Airplane Design Specifications, to be published later.

signed for exhibition purposes, and deserve closer attention in the future.

To increase the reliability of airplanes which have not sufficient gust resistance, according to the present stage of knowledge, it is necessary to limit the speed of such airplanes by a warning sign on the instrument board, such as is customary in all public vehicles of transportation.

f) The dynamic stress on tail surfaces in gusts can be computed in the same way as for the airplane wings by substituting the mass $m_r = (m i^2)/(a^2 + i^2)$ reduced to the neutral point of the control surface for the total mass of the airplane; a here denotes the distance of the neutral point from the center of gravity and i the radius of inertia. The C.I.N.A. (International Commission for Aerial Navigation) proposes for the dynamical surface loading of the vertical tail group the formula $p_s = 3.6 v_h$ (kg/m^2), that is, exactly as above, a stress linearly dependent on the flight speed.

g) If the gust stresses of an airplane flying level at cruising speed are already of noticeable magnitude, they increase to wing failure when the airplane, through some cause (error in piloting, nonvisibility in clouds, etc.), gets into a vertical glide and the air speed increases. It is then that

1. Comparatively slight gust impacts can induce wing failure.
2. Pull-up accelerations familiar to the pilot and harmless in calm air, can multiply to breaking stresses in a slight gust.

It should be impressed upon the pilot to avoid all speed increases and pull-up maneuvers in gusty weather. Experienced pilots do not attempt to fight against gusts by elevator or aileron, but allow the airplane to swing back of its own accord into its normal flight attitude through its natural stability, and merely apply the rudder to keep the course.

Translation by J. Vanier,
National Advisory Committee
for Aeronautics.

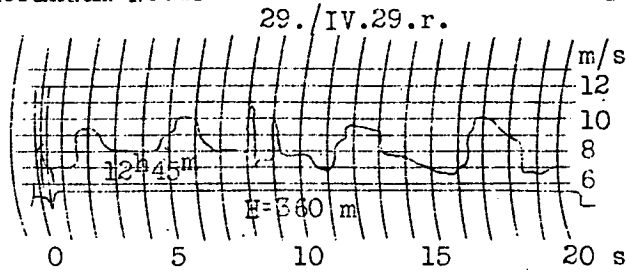


Fig.1 Gust record taken with Kite instrument.

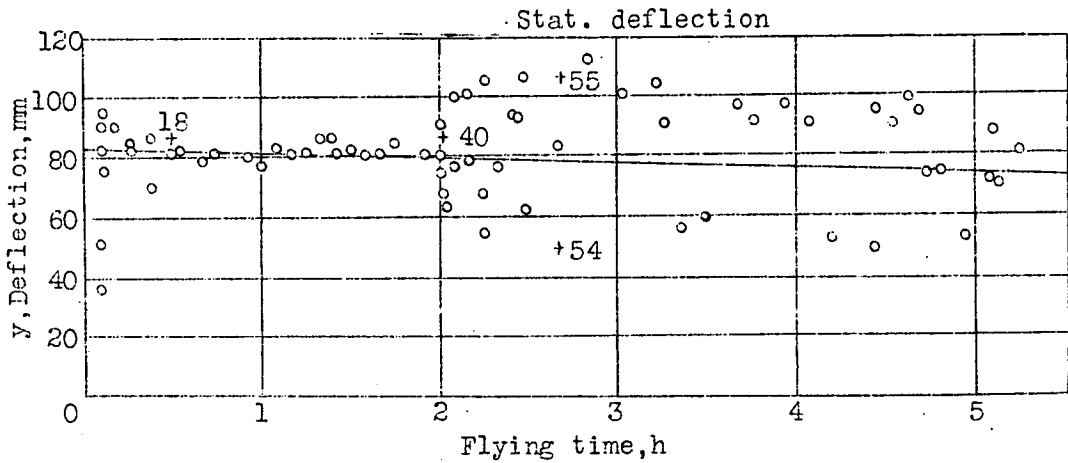
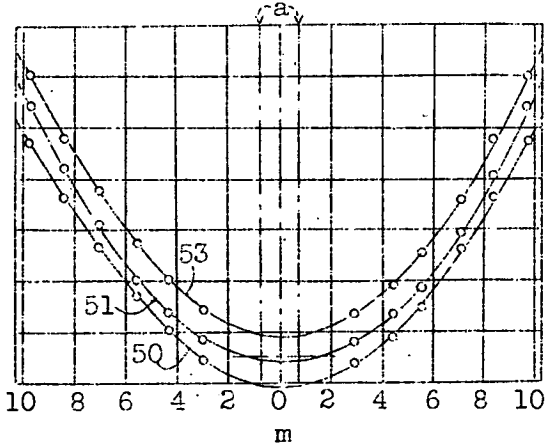
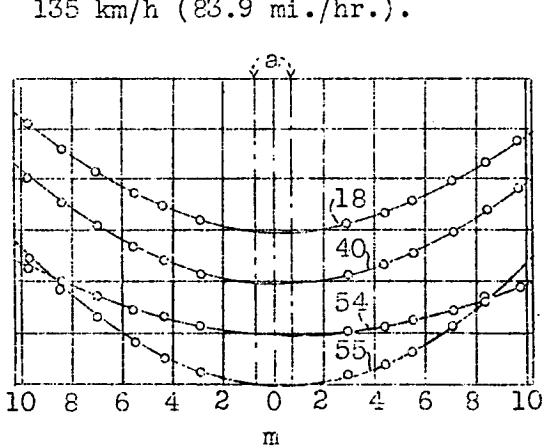


Fig.3 Deflection y of starboard wing. (M-24) 9.45 m (31.0 ft.) from the fuselage center during a cross-country flight. Weight at take-off 2.44 t (5379.2 lb.), at landing 2.17 t (4784 lb.), speed = 135 km/h (83.9 mi./hr.).



a, Wing fitting to fuselage.

Fig.4 Deflection curve in free flight of M-24 wing. (1.57 in.) Scale of ordinates: 1 unit = 40 mm deflection. (From flight Fig.3)

Fig.5 Deflection curves of M-24 wings in gusts extrapolated for same starboard tip deflection. (From flight Fig.3 Gross weight = 2.31 t (5092.7 lb.))

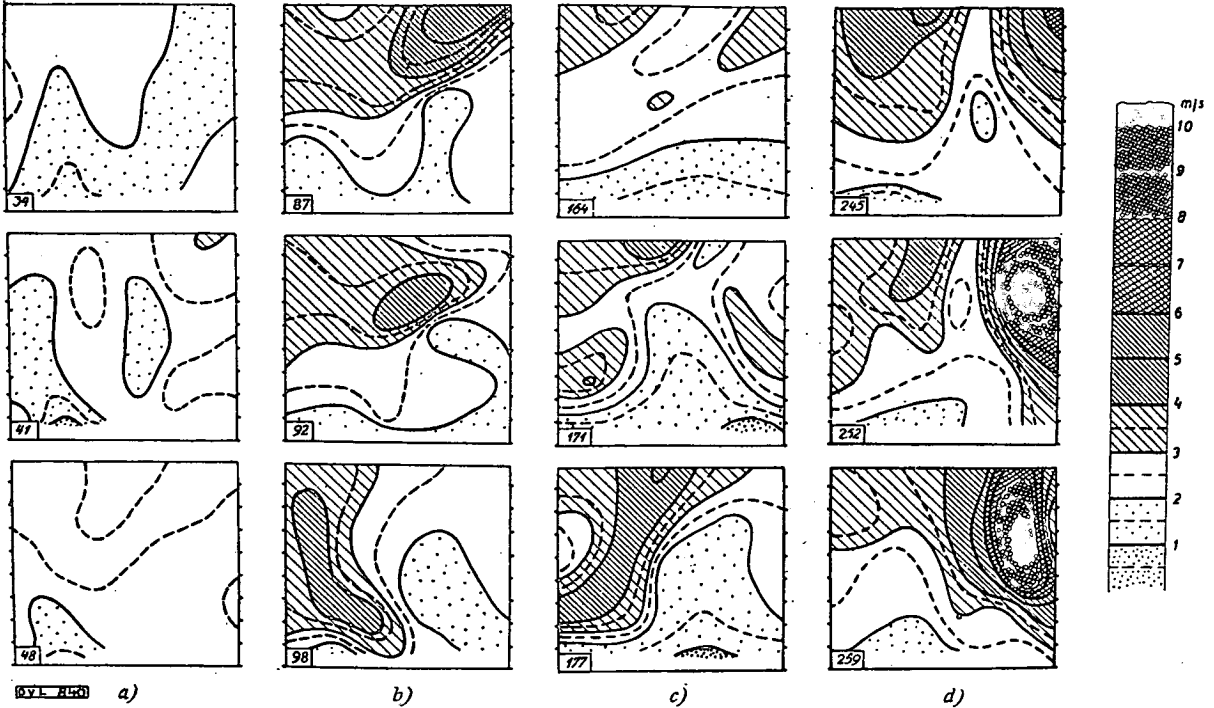


Fig.2 Gust structures. Each picture represents a field 10 x 10 m (32.8 x 32.8 ft.) explored at 25 test stations. Each set of three pictures follows at 1 sec. interval. The hatchings denote wind velocities, and are explained on the margin.

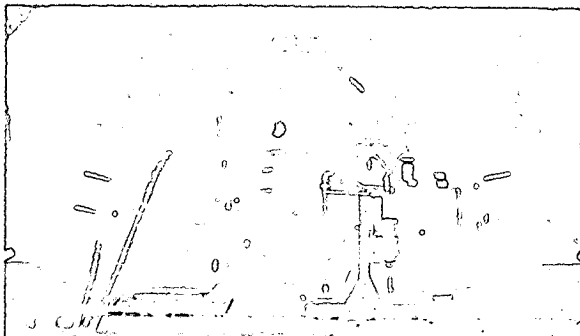


Fig.13 Installation of optograph in fuselage of M 24 for measuring wing deflection.

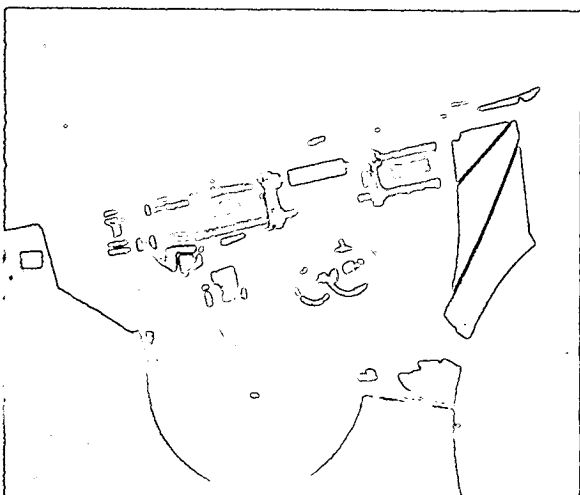


Fig.23 Optograph mounted below fuselage of Junkers F 13 for recording wing stresses in free flight.

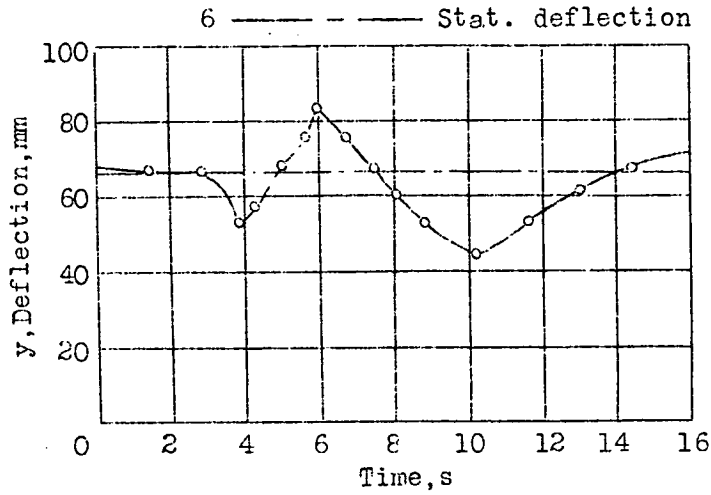


Fig.6

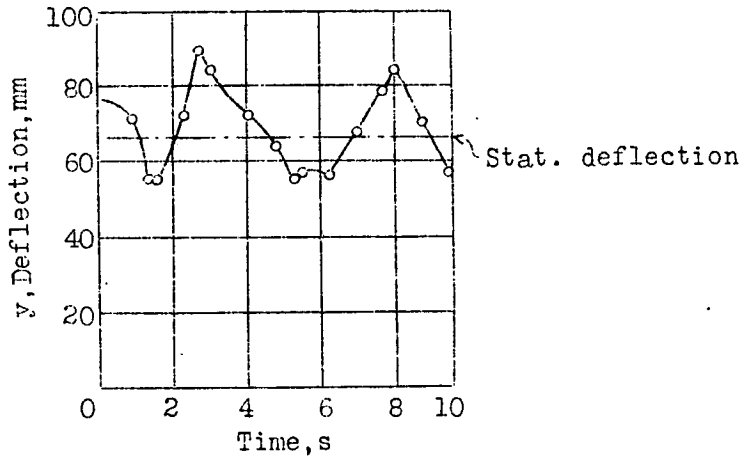


Fig.7

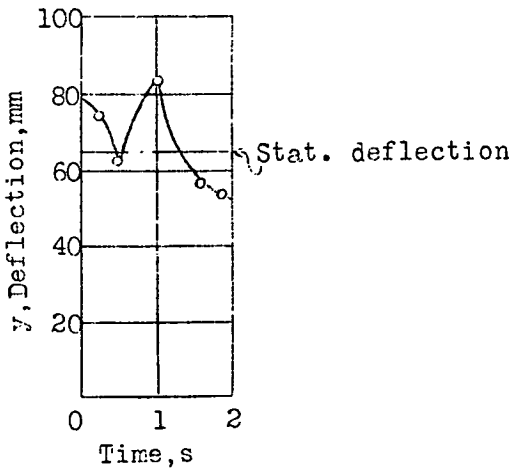


Fig.8

Figs.6,7,8 Deflection y of M-24 starboard wing (9.45 m (31 ft.) from fuselage center) in gusts. (From flight Fig.3, gross weight ~ 2.3 t (5070.6 lb.))

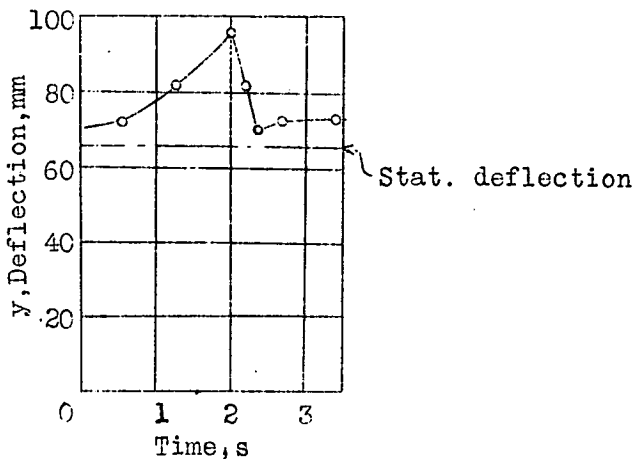


Fig.9

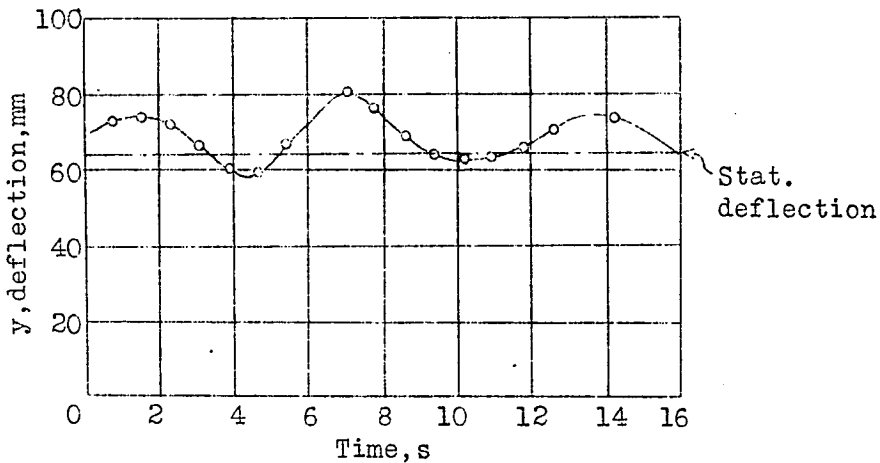


Fig.10

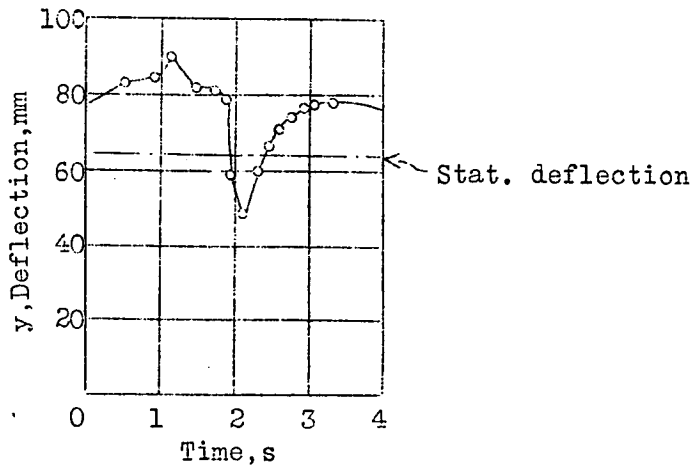


Fig.11

Fig.9,10,11 Deflection y of M-24 starboard wing (9.45 m (31 ft.) from fuselage center) in gusts. (From flight Fig.3, gross weight ~ 2.3 t (5670.6 lb.))

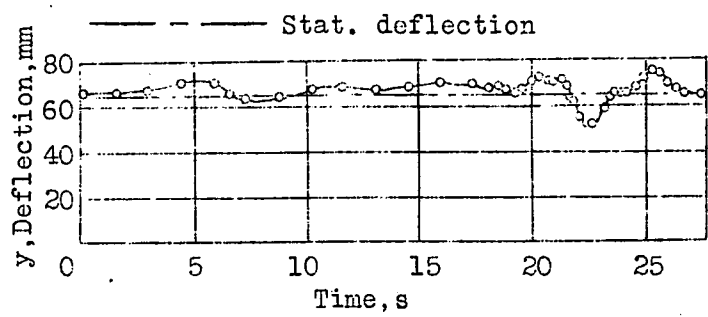


Fig.12a

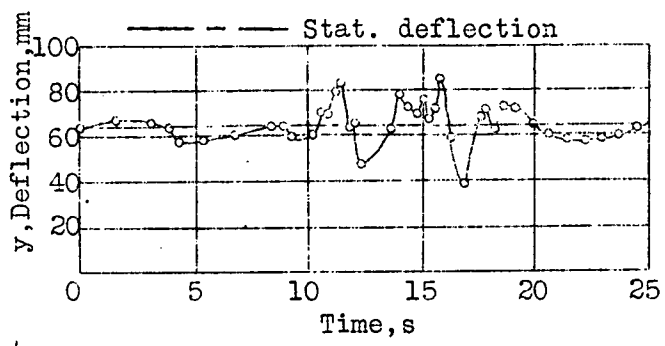


Fig.12b

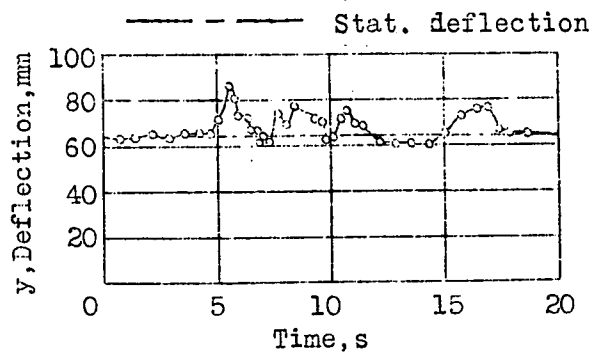


Fig.12c

Figs.12a,12b,12c Deflection y of M-24 starboard wing(9.45 m (31 ft.) from fuselage center) in gusts. (From flight Fig.3, gross weight \sim 2.3 t (5070.6 lb.).)

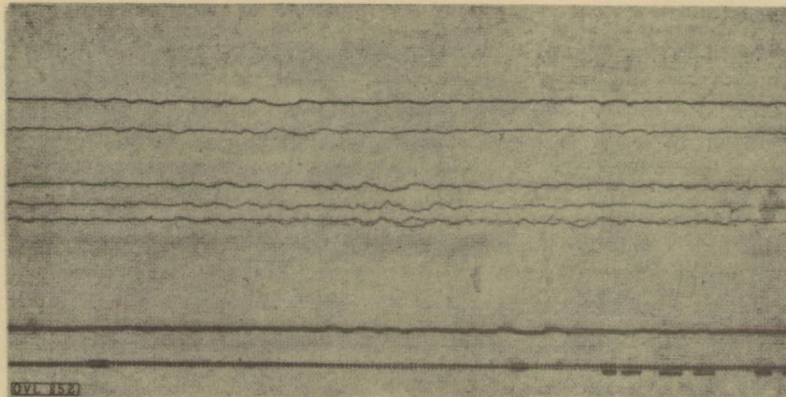


Fig.14 Gusts over Thüringer forest. $v = 135 \text{ km/h}$ (83.9 mi./hr.). Gross weight = 2.34 t (5158.8 lb.)

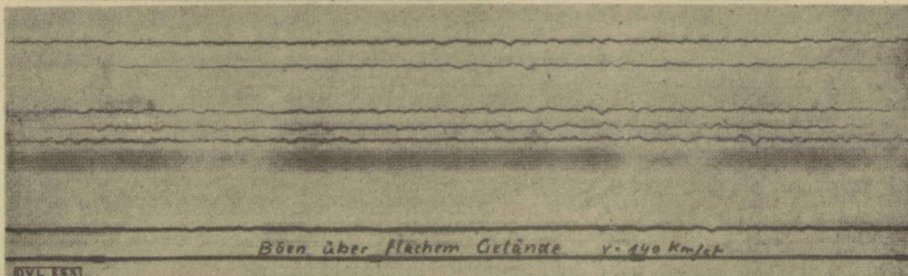


Fig.15 Gusts over flat terrain. $v = 140 \text{ km/h}$ (86.99 mi./hr.) Gross weight = 2.30 t (5070.6 lb.)

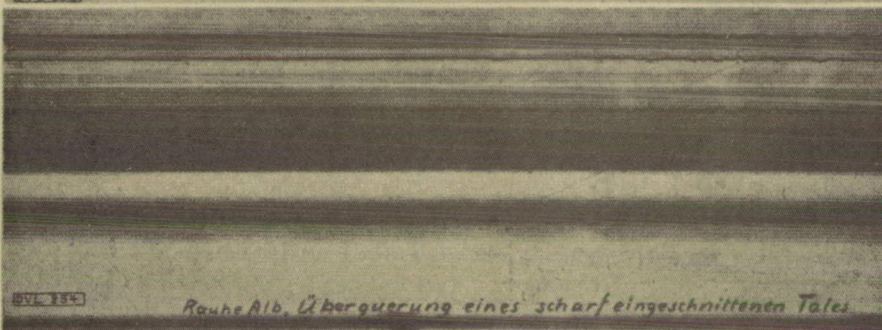


Fig.16 Rauhe Alb, crossing a sharply indented valley. $v = 135 \text{ km/h}$ (83.9 mi./hr.) Gross weight = 2.35 t (4960.4 lb.)

Figs.14,15,16 Optograms of M 24 port wing. The black lines are traces of lamps distributed over the wing. Time and Morse marks at lower edge, interval of time marks 0.6 sec., each minute a long dash.

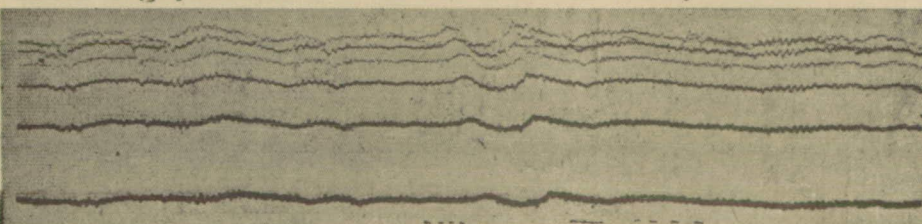


Fig.24 Sun gusts over lakes near Potsdam at 300 m altitude. (984 ft.) $v = 135 \text{ km/h}$

(83.9 mi./hr.) Gross weight = 1.8 t (3968.3 lb.)

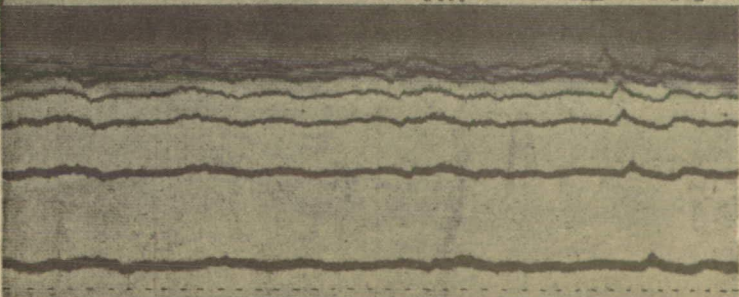


Fig.25 Gusts just preceding landing. $v = 135 \text{ km/h}$ (83.9 mi./hr.) Gross weight = 1.8 t (3968.3 lb.)

Figs.24,25 Optograms of F 13 starboard wing. The dashes are lamp traces, time and Morse marks at lower margin.

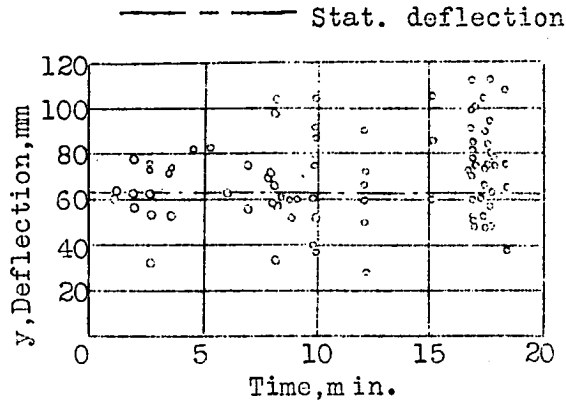


Fig.17 Deflection y of F 13 starboard wing(8.85 m (29.04 ft.) from fuselage center) during flight. Gross weight = 1.8 t (3968.3 lb.) v = 130 km/h (80.8 mi./hr.)

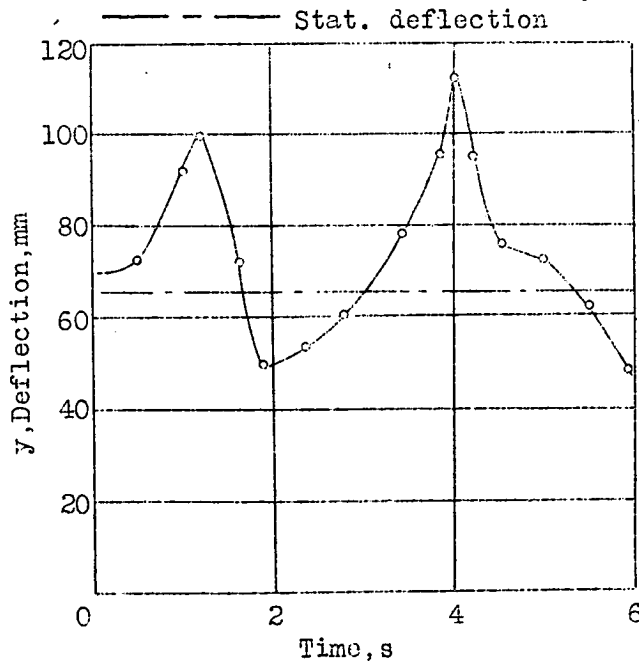


Fig.18 Deflection y of F 13 starboard wing in gusts. 8.85 m (29.04 ft.) from center of fuselage. Gross weight =1.8 t (3968.3 lb.) v = 130 km/h (80.8 mi./hr.).

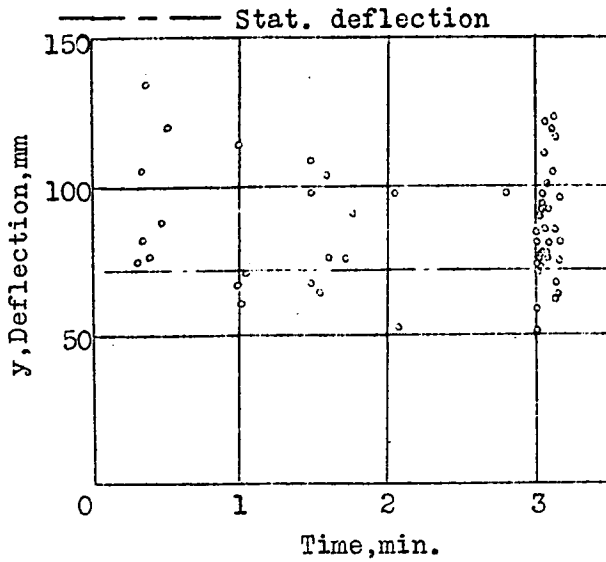


Fig.19

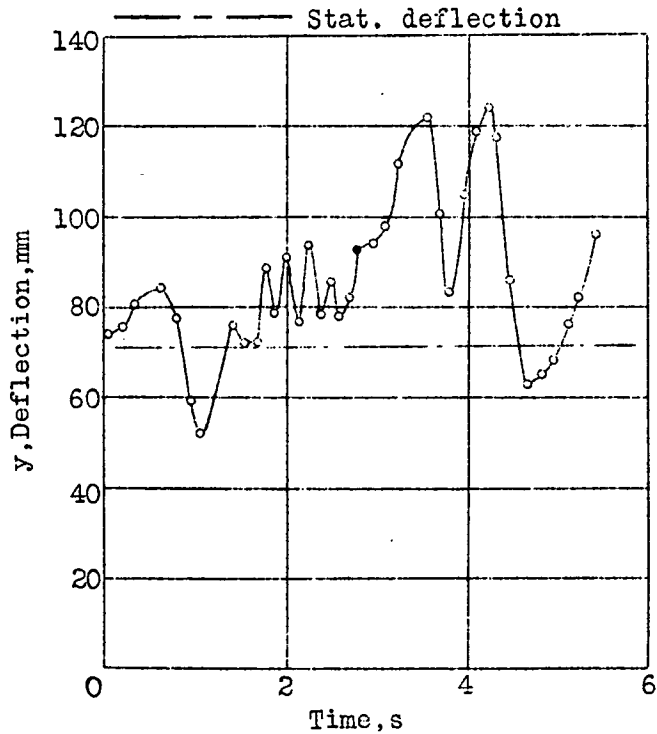


Fig.20

Figs.19,20 Deflection y of F 13 starboard wing in gusts. 8.85 m (29.04 ft.) from center of fuselage. Gross weight=1.8 t (3968.3 lb.) $v = 130$ km/h (80.8 mi./hr.).

c, Plane of ground - glass plate
d, Fuselage junction

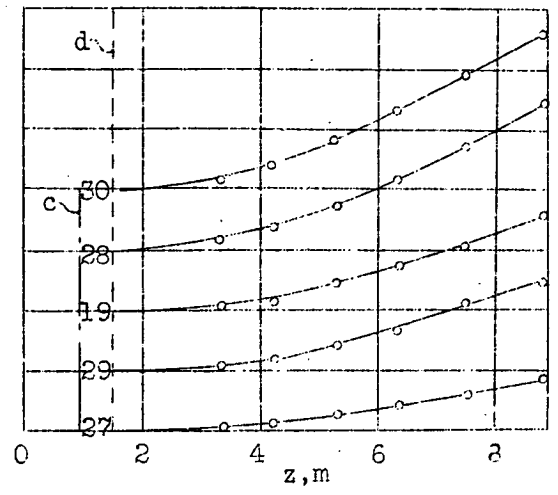


Fig.21 Deflection curves recorded in free flight on F 13 wing.
(Ordinate scale:1 unit = 50 mm (1.97 in.) deflection.
Gross weight = 1.8 t (3968.3 lb.) v = 130 km/h (80.8 mi./hr.).

c,Plane of ground
-glass plate.
d,Fuselage
junction

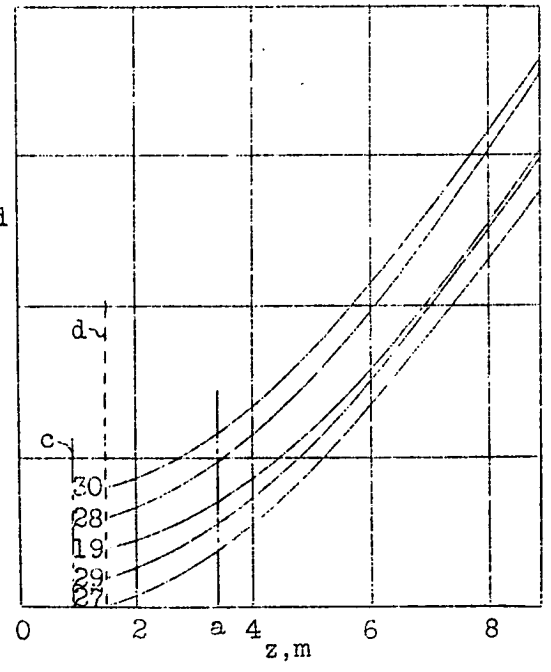


Fig.22 Deflection curves of Fig.21 extrapolated for same curvature
by z = a .

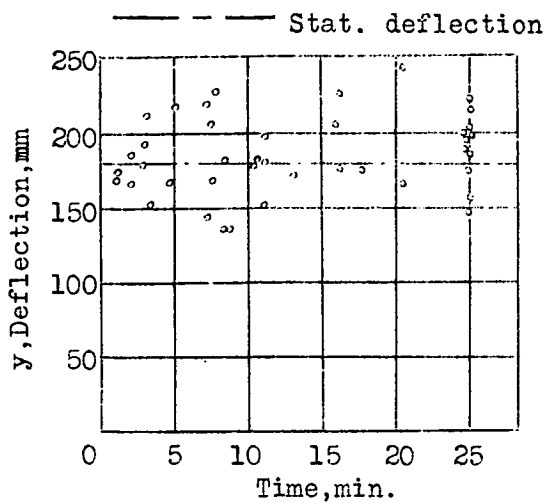


Fig.26 Deflection y of starboard wing tips of G 24. Gross weight= 4.7 t (10361.7 lb.) v = 125 km/h (77.7 mi./hr.).

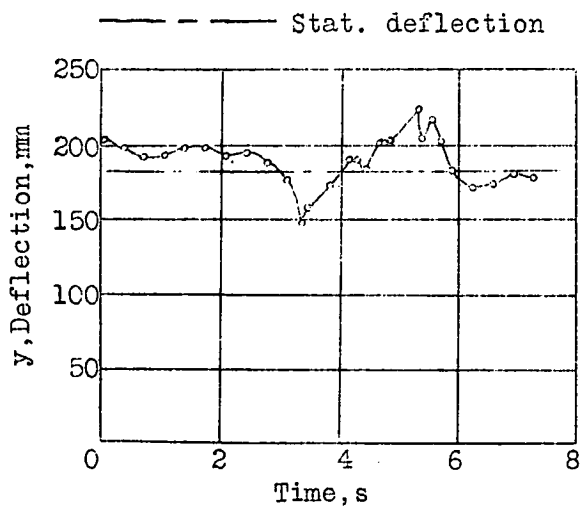


Fig.27 Deflection y of G 24 starboard wing in a gust.

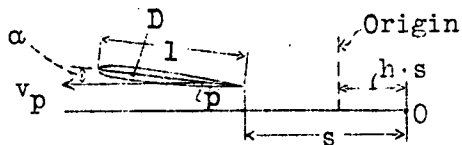


Fig. 28 Unsteadily moved wing.

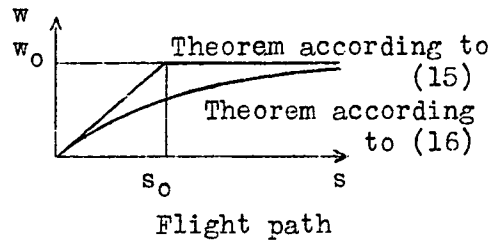
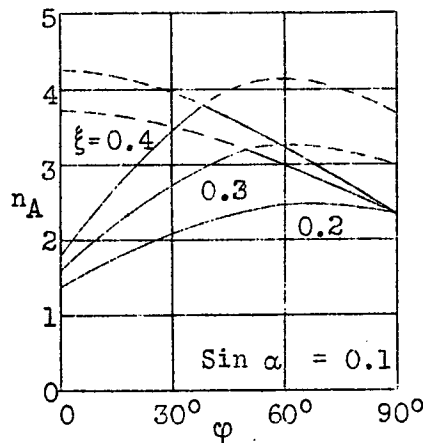
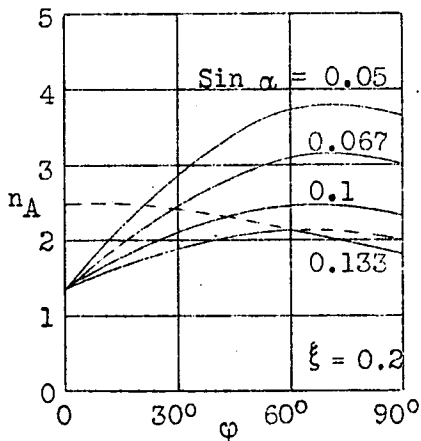


Fig. 31 Gust velocity w against flight path.



Figs. 29,30 Load factor n_A for case A for airplanes in gusts for different angles of gust φ plotted against flight path.
 α = angle of attack, ξ = ratio of gust to flight velocity; separation occurs at sine $\alpha = 0.3$

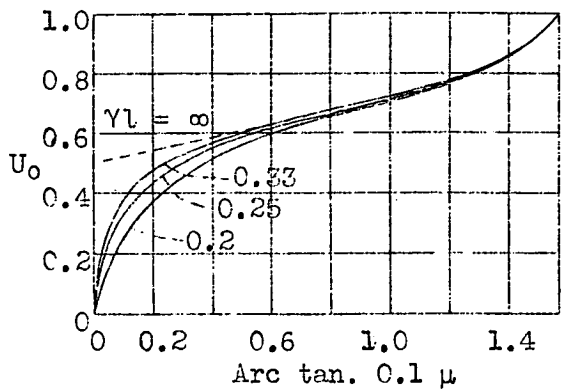


Fig. 32 By linear rise in velocity.

Figs. 32,33 Ratio of stress U_0 in vertical gust to mass μ , plotted against gust gradient γ .

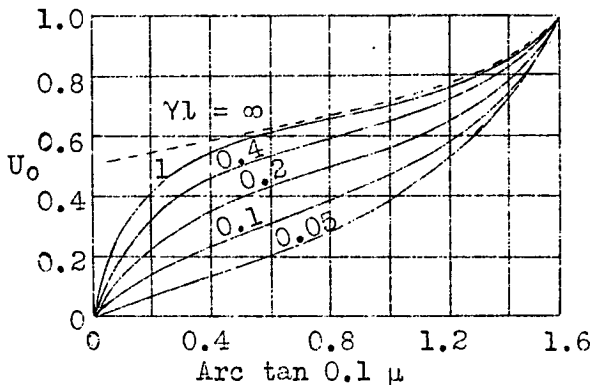


Fig. 33 By asymptotic rise of velocity.

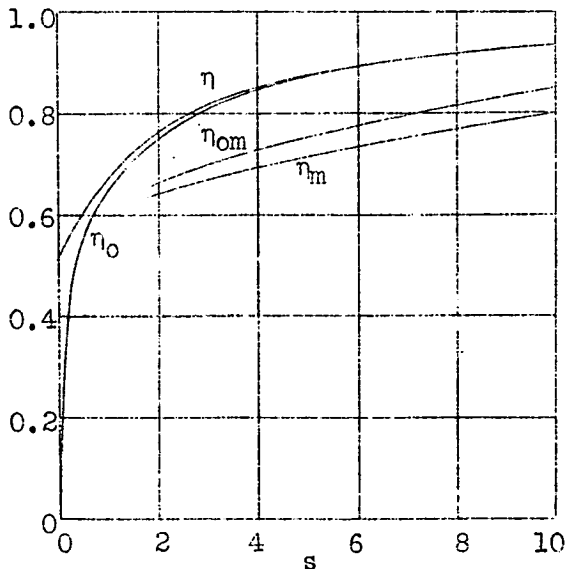


Fig. 34 Lift factors η and η_0 and their averages over flight path s (in units of chord)

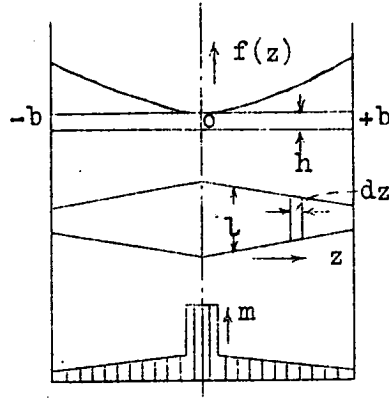
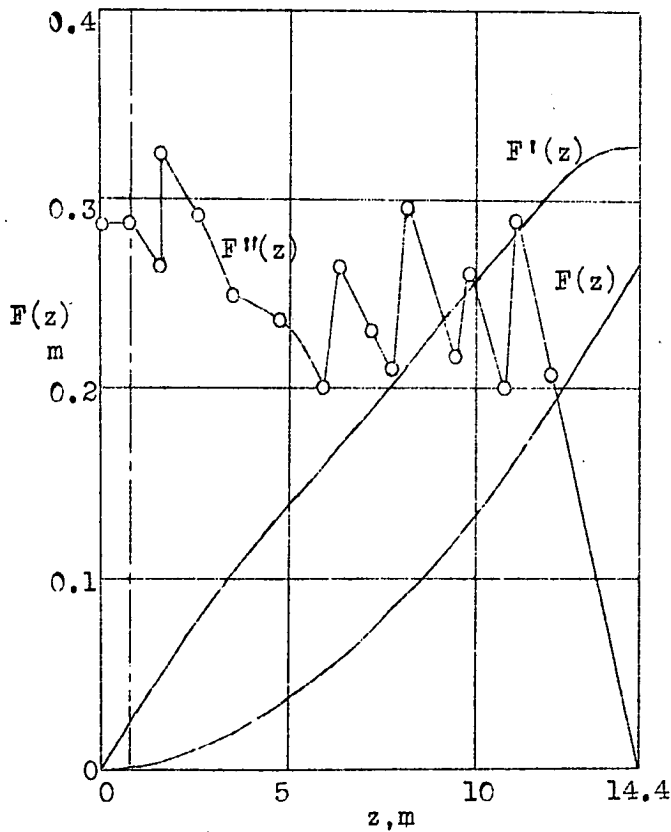


Fig. 35 Deflection curve and mass distribution of airplane wing.



Fig, 36 Statical deflection curve $F(z)$ of G 24 wing.

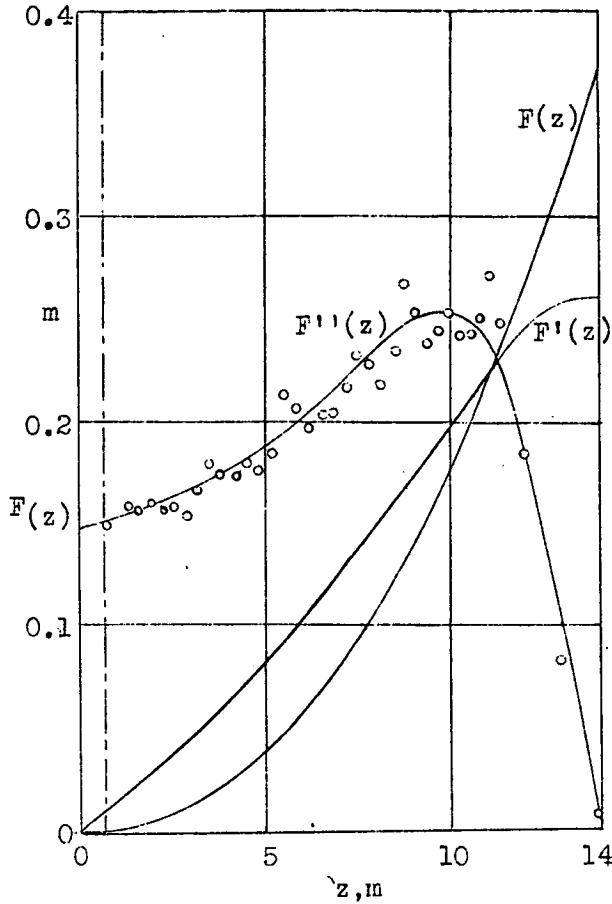


Fig. 37 Static deflection curve $F(z)$ of J 49 wing.

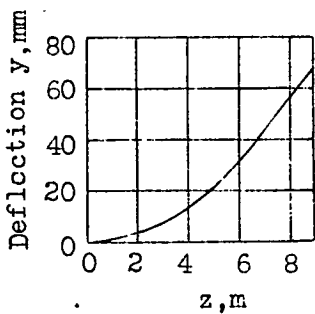


Fig. 38 Static deflection curve of F 13 in flight. (1.79 t) or 3946 lb.)

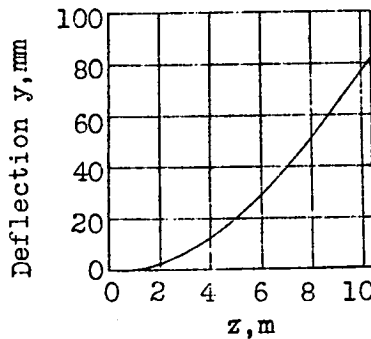


Fig. 39 Static deflection curve of M 24 in flight. (2.43 t) or (5357 lb.)

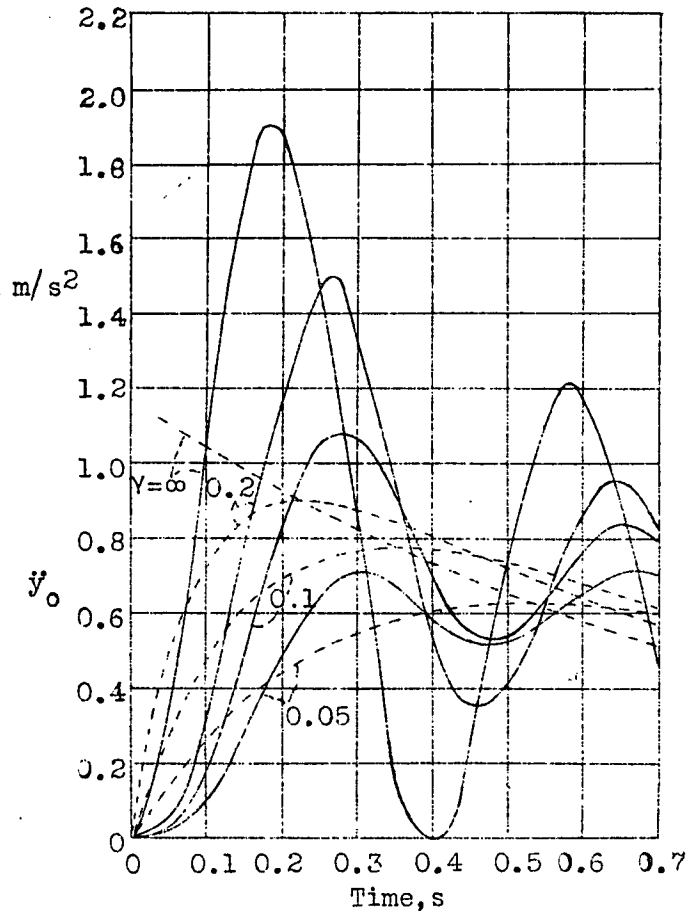


Fig. 40 Junkers G 24

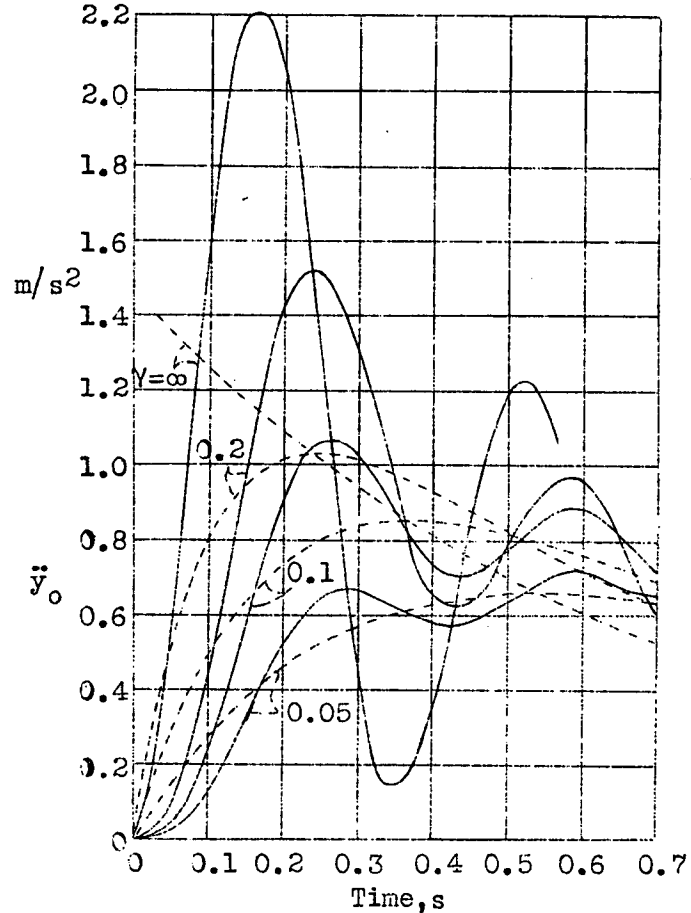


Fig. 41 Junkers J 49

Figs. 40,41 Time rate of stresses of elastic (full line) and rigid(dash line) wings in vertical gusts with asymptotic rise of velocity, plotted against gust gradient γ . vertical velocity with $\infty w_0 = 1 \text{ m/s}$ (3.28 ft./sec.)

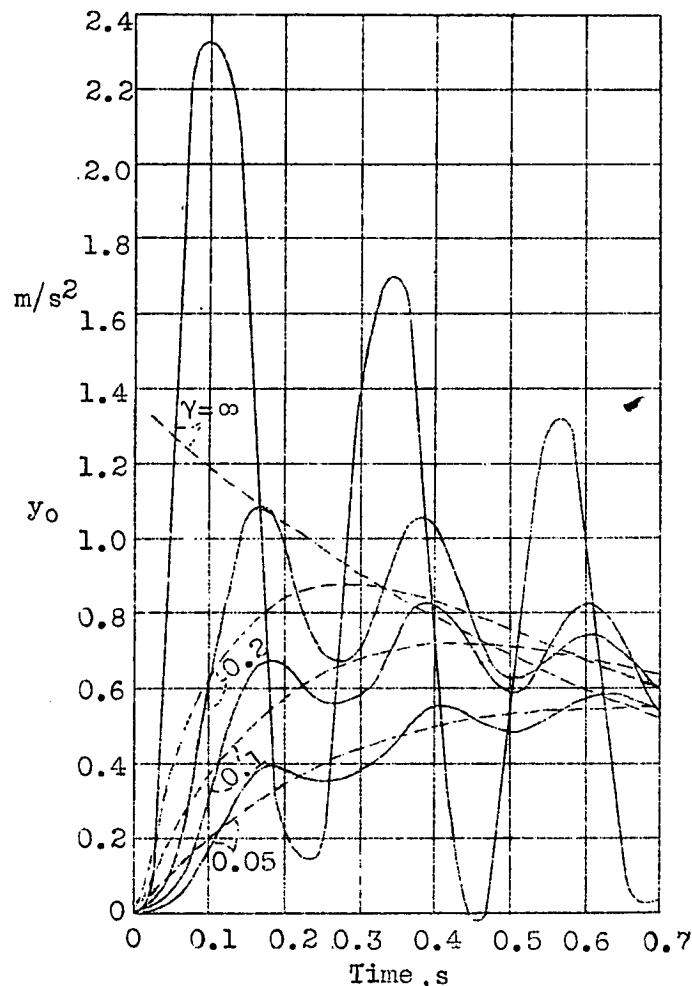


Fig. 42 Junkers F 13

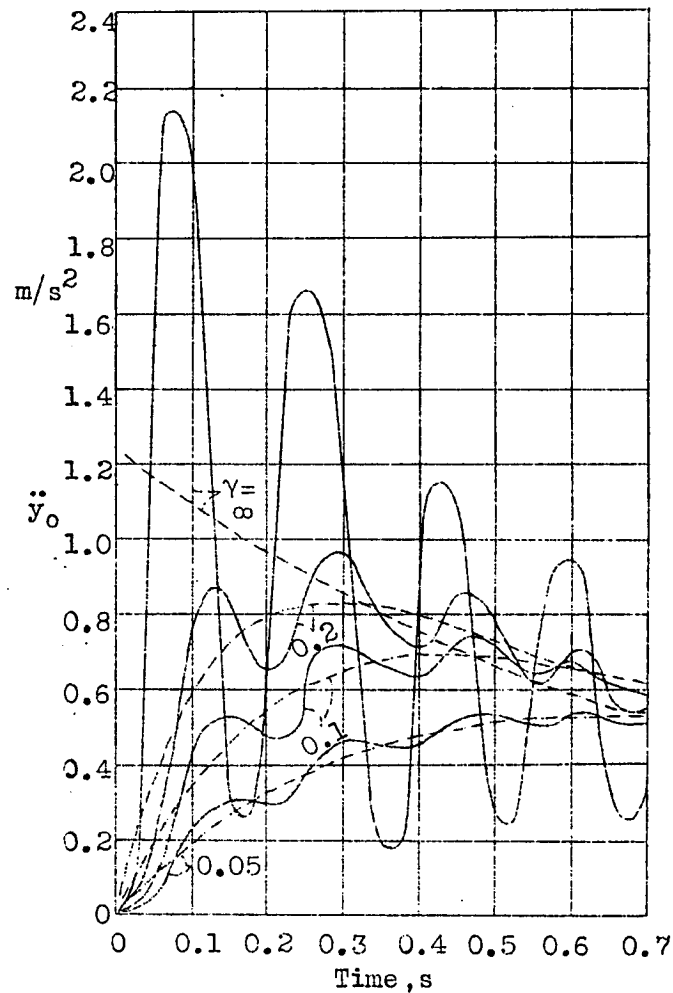


Fig. 43 Messerschmitt M 24

Figs. 42,43 Time rate of stresses of elastic (full line) and rigid (dash line) wings in vertical gusts with asymptotic rise of velocity, plotted against gust gradient γ , vertical velocity with $\infty w_0 = 1 m/s$ (3,28 ft./sec.)

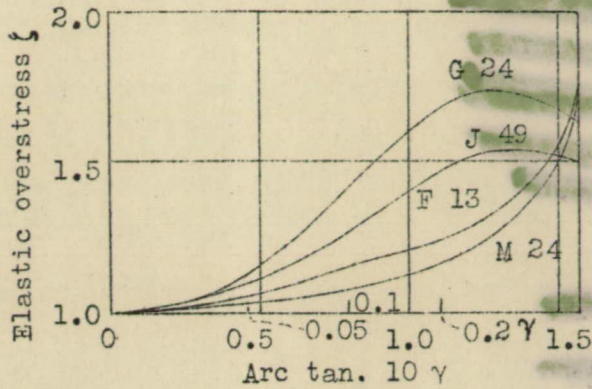


Fig. 44 Ratio of gust stresses in the elastic to the rigid wing of the four airplanes plotted against gust gradient γ .

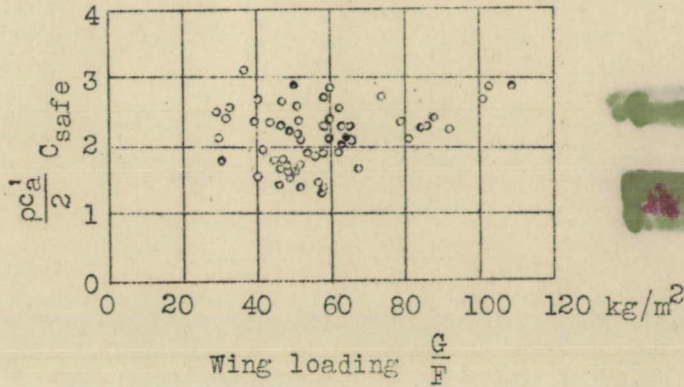


Fig. 45 Gust resistance of German airplane.

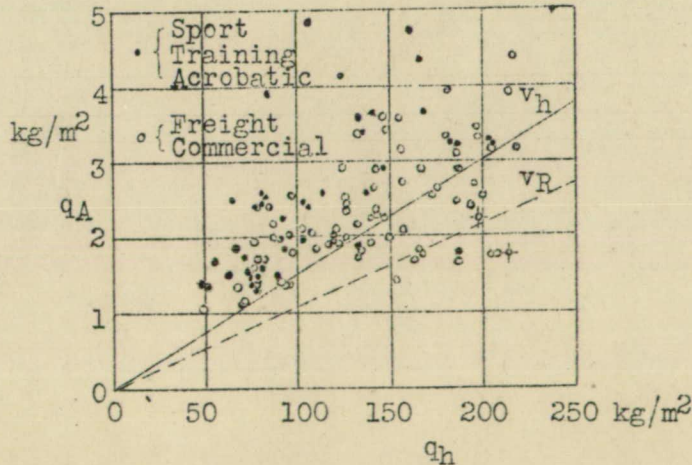


Fig. 46 Dynamic pressure at failure q_A of German airplanes.

v_h = maxim. level flight.
 v_R = cruising speed.